Dynamical properties of the normal phase of betaine calcium chloride dihydrate. II. A semimicroscopic model

1996 J. Phys.: Condens. Matter 8 8221

(http://iopscience.iop.org/0953-8984/8/43/017)

J. Phys.: Condens. Matter **8** (1996) 8221–8250. Printed in the UK

Dynamical properties of the normal phase of betaine calcium chloride dihydrate. II. A semimicroscopic model

J Hlinka†, M Quilichini†, R Currat‡ and J F Legrand‡

† Laboratoire Léon Brillouin, Centre d'Etudes de Saclay, Gif-sur-Yvette, France
‡ Institute Laue-Langevin, 38042 Grenoble, France

Received 22 April 1996

Abstract. A ten-parameter quasi-harmonic semimicroscopic model for the low-frequency lattice dynamics of betaine calcium chloride dihydrate is presented. The choice of the relevant variables and interaction terms of the model potential is mainly based on the known crystallographic data, while the values of the quasi-harmonic force constant parameters are adjusted to our recent inelastic neutron scattering data. The parameter with the largest temperature derivative is determined and the origin of its temperature renormalization is discussed.

1. Introduction

It is now admitted that the general origin of incommensurability in insulators consists in the competition of interactions or in the competition of periodicities which are favoured by these interactions. To a large extent this understanding is due to the introduction and exhaustive investigation of simple models such as the Frenkel–Kontorova [1] (see also [2, 3]), ANNNI [4, 5] and DIFFOUR [6] models. All these models account not only for the existence of the incommensurate phases but also for the existence of a sequence of commensurate phases, as found experimentally in the phase diagram of betaine calcium chloride dihydrate (BCCD).

Tentrup and Siems [7] proposed to map the experimental P–T phase diagram of BCCD onto the well established phase diagram of the ANNNI model. Their main assumption was that the unknown physical quantity, which in this mapping is identified with the ratio J_1/J_2 of first- to second-neighbour interactions, depends on temperature and pressure only through the average lattice constant. The success of their approach proves that the general hypothesis that such a mapping should exist is correct. On the other hand, because of the lack of explicit microscopic interpretation for the ANNNI model pseudo-spin variables, and also because there is no provision for pseudo-spin dynamics in this model, the possibility of relating the effective values of the J_1/J_2 ratio to other properties of BCCD is quite limited.

The DIFFOUR model is conceptually much closer to usual lattice dynamical models, because it is based on the interaction potential expressed in terms of continuous positional variables of particles forming a discrete periodic array. Chen and Walker [8] have proposed a model of this type for BCCD. They propose to associate each atom in the unit cell with one of the two σ_c planes at $c = \frac{1}{4}$ and $c = \frac{3}{4}$ and to ascribe two local variables to each so-defined 'layer'. Moreover, in order to relate the possible equilibrium configurations of their model to the known space group symmetry of the various BCCD phases, they

0953-8984/96/438221+30$19.50

attributed appropriate symmetry properties to their variables. For each layer, one variable is symmetric and one antisymmetric with respect to the σ_c plane associated with the layer. Furthermore, all variables are antisymmetric with respect to the σ_b plane in order to allow the construction of three-dimensional displacement waves having the symmetry of the order parameter, as proposed by Ao and Schaack [9] and established by Perez-Mato [10].

Further progress was achieved via a closer identification of the atomic displacements involved in the modulation, and their relation to the observed phonon modes. Two kinds of characteristic displacement were identified.

First, the structure refinement of the normal phase performed by Brill *et al* [11] revealed large anisotropic librations of the betaine molecules and also of the 'Ca complexes', each around its own particular axis in the σ_b plane. Dvořák [12] suggested that these large librations could be associated with the lowest-frequency Raman- [9] and infrared-active [13–15] modes. He proposed to take these librations as critical degrees of freedom relevant to the phase transition and suggested the construction of a DIFFOUR-type model with variables describing correlated librations of the betaine and Ca octahedra.

The importance of including the translational degrees of freedom was recognized after the inelastic neutron scattering work of Currat *et al* [16]. Their results showed that the transition to the incommensurate phase is accompanied by phonon softening and that the soft mode belongs to a mixed acoustic–optic branch. This implies that there are translational contributions to the soft-mode eigenvector. Furthermore, the mixed translational–rotational character of the static displacement modulation pattern was evidenced by the structure refinement of Zuñiga *et al* [17].

The coupling between acoustic and optic branches was initially proposed as a possible origin for an incommensurate instability by Axe *et al* [18] in 1970. Since then this type of mechanism was evidenced in two incommensurate insulators: quartz and K_2SeO_4.

The anomalous character of the observed phonon dispersion branches allowed one in some cases to construct quantitative phenomenological mode-coupling models, in which the phonon eigenmodes are obtained via a diagonalization of a mode-mixing matrix, written in terms of a conveniently chosen set of 'bare' modes. The numerical values of the parameters entering the mode-mixing matrix are determined by fitting to the experimental phonon dispersions.

The work of Axe *et al* [18] on $KTaO_3$ and of Dolino *et al* [19, 20] on quartz illustrate this approach. For these two cases the anomaly was located in the very vicinity of the zone centre. In this case the development of the bare branches (and of their mutual interaction) in powers of the phonon wavevector q can be used as a convenient way to parametrize the dynamical matrix.

This approach clearly cannot be used when the dispersion anomaly is located deep inside the Brillouin zone such as for K_2SeO_4. Instead, the development in Fourier series must be used. This is justified for most insulators, because the limitation of the Fourier development of the bare mode dispersion to the first few terms corresponds physically to the approximation of short-range interactions. A simple mode-mixing model of this type was recently proposed by Pérez-Mato [25] for K_2SeO_4.

Still, it should be stressed that in both of the above-mentioned models (quartz and K_2SeO_4) the assumptions that go beyond a simple *first-neighbour acoustic–optic interaction approximation* are crucial. In the K_2SeO_4 case, the minimum on the soft-mode branch appeared only after including a term describing the interaction between the 'optic' and 'acoustic' degrees of freedom associated with *second-neighbour* sites. Similarly, the model for quartz would not account for the incommensurate instability if the fourth-order term hq^4 in the parametrization of the soft branch were omitted. It will be shown in this paper that the

coupling to a second optic branch is most likely to be at the origin of the incommensurate character of the instability in BCCD.

Thus phenomenological mode-coupling models are useful not only because they enable one to account for the anomalous variation in the frequencies, structure factors and damping constants of the mixed modes as a function of q, but also because they may provide a closer understanding of the origin of incommensurability in these crystals.

In the preceding paper, part I [21], we presented the results of a detailed inelastic neutron study of the dispersion curves in deuterated BCCD. These measurements were performed in order to set up a quantitative mode-coupling model applicable to BCCD. However, we have found that, owing to the existence of two closely spaced optic branches, a purely *phenomenological* approach does not allow an unambiguous determination of the mode mixing matrix. Therefore, we developed instead a semimicroscopic model in which the parametrization of the mode-mixing matrix is directly derived from arguments based on structural and dynamical data.

In the meantime, Kappler and Walker [22] modified their original model in order to reach agreement with the measured dispersion curves [16], by including the acoustic branch. They have found that a rich sequence of modulated phases, similar to that observed experimentally, can be obtained equally well in the modified model as in their previous model which do not include coupling to the acoustic branch. Obviously, the model that we propose here is in several respects similar to that of Kappler and Walker. However, the work in [16] is centred on the determination of the phase diagram, while in this contribution we are concerned with the definition and the physical interpretation of the model itself. Such an interpretation is necessary in order to allow a direct comparison of the model with as many experimental results as possible.

In section 2.2 below, we define a set of convenient local variables and in section 2.3 we describe explicitly the approximations which are used to obtain the general form of the quasi-harmonic potential. In section 3 the symmetry-adapted bare modes are introduced and the properties of the corresponding mode-mixing matrix are analysed. The possibility of adjusting the values of the ten model parameters on the experimental phonon dispersion curves is discussed in section 4. Then the model is used to study the temperature dependence of the phonon dispersions and the possible role of various anharmonic terms is considered. Finally, section 5 is devoted to the discussion of the results and to possible improvements to the present model.

2. Definition of the model

2.1. General assumptions

For crystals composed of well defined rigid entities, the eigenvectors of the lowest branches represent essentially rotations and translations of each entity as a whole. The dispersion of these branches may then be calculated from rigid-body models, in which the internal degrees of freedom are not taken into account. On the basis of the available structural data, we expect that for BCCD the betaine molecules and to some extent also the Ca complexes $CaCl_2 \cdot 2H_2O$ could be treated as such rigid units.

Another simplification of the problem can be achieved, if phonon dispersions are calculated only along directions or planes of special symmetry. In this case the dynamical matrix may be converted into a block diagonal form, where each block corresponds to a different symmetry representation and can be diagonalized separately. In BCCD the soft phonon belongs to the Λ_3 representation, which has eigenvectors antisymmetric with respect

to the mirror plane σ_b. Therefore only those degrees of freedom that are antisymmetric with respect to σ_b are introduced here. Consequently, only the phonons propagating in the a^*–c^* plane can be calculated, as for a general propagation direction out of this plane the phonon eigenvectors contain both σ_b-symmetric and σ_b-antisymmetric contributions.

The restriction to the σ_b-antisymmetric rigid-body degrees of freedom leaves us with three degrees of freedom (translation T_y and rotations R_x and R_z) per rigid-body unit. In the following, still more drastic simplifications will be made, as we shall retain only one translational and one rotational degree of freedom per whole formula unit of BCCD.

Such an approach will enable us to derive a simple lattice dynamical (quasi-harmonic) model which we shall later use as a basis for developing a DIFFOUR-type anharmonic model [23].

2.2. Relevant variables

There are four formula units per unit cell of BCCD. Taking the basic formula unit as defined by Brill *et al* [11], the other three units may be deduced by symmetry operations. Each formula unit has a mirror symmetry element, coinciding with a σ_b plane of the Pnma structure. The basic formula unit and the unit related by σ_c can be associated with the σ_b plane at $y = \frac{1}{4}$ and the other two formula units with the σ_b plane at $y = \frac{3}{4}$ (figure 1).

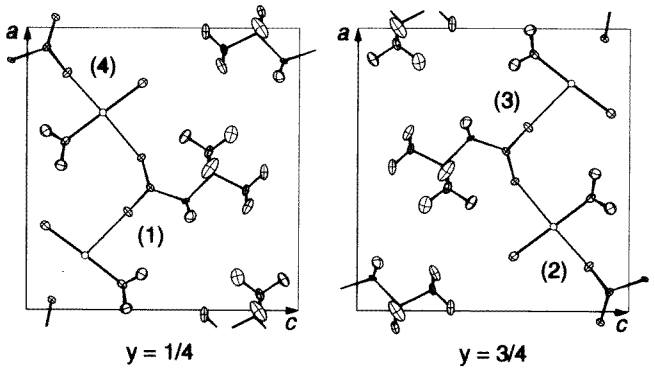

(a) (b)

Figure 1. There are four formula units per unit cell of BCCD, (a) two related by the σ_b plane at $y = \frac{1}{4}$ and (b) the other two by the σ_b plane at $y = \frac{3}{4}$. Labels 1–4 are defined in the text (see section 2.2).

In the following the four formula units of the primitive unit cell, deduced by E, σ_a, C_{2y} and σ_c, from the basic unit, will be indexed as 1, 2, 3 and 4, respectively.

The TLS analysis of the thermal Debye–Waller factors [11] shows that the characteristic degrees of freedom of the soft-phonon branch are the rotations of both entities (Ca complex and betaine molecule), each around its own preferential axis lying in the corresponding (σ_b) mirror plane. The structure analysis of the modulated phases [17, 36] confirmed that essentially the same rotational distortions appear in the frozen modulation pattern. Let us refer to the rotations of these entities around their preferential axes as the 'easy rotations'. All the other rotational degrees of freedom will be neglected.

Further, from the geometry of the atomic displacements involved in the easy rotations (figure 2), one may expect that the coupling between the easy rotation of each betaine

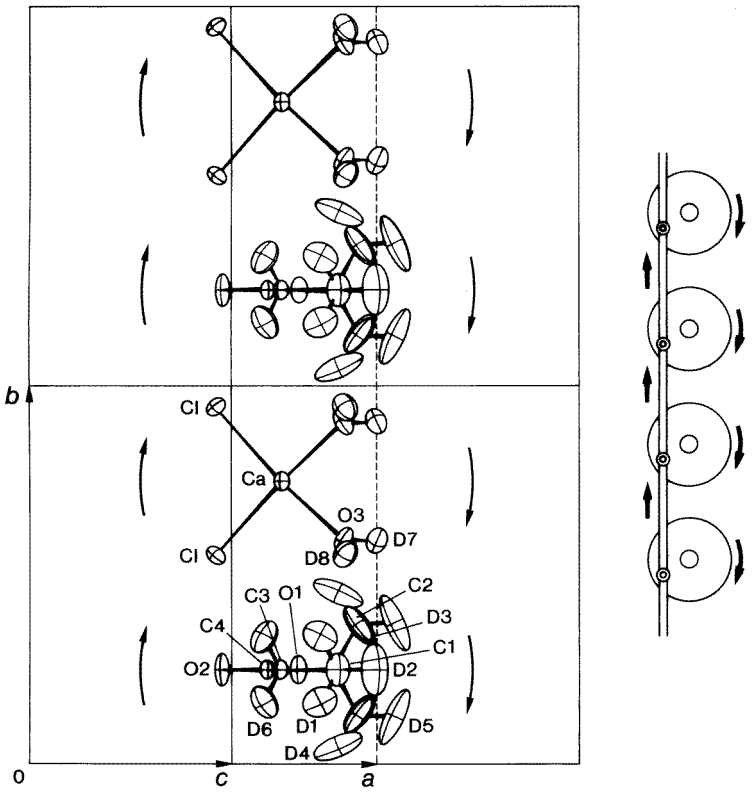

Figure 2. The 'column'. Top: the betaine molecules and Ca complexes ($CaCl_2 \cdot 2H_2O$) belonging to the same 'column' A_{00} viewed along the axis of rotation. The thermal ellipsoids have their longest axes oriented tangentially to the axis of 'easy rotation'. The *b* axis is vertical. Bottom: schematic representation of the mutual correlations of the easy rotations inside the column. The structure refinement of the modulated phase [17] shows that the static displacements of the betaines and Ca complexes inside the same column are oriented in the same sense, as if linked by connecting rods.

molecule with its nearest-neighbour Ca complexes along the *b* direction is larger than the couplings with its 'transverse' neighbours (lying in the same σ_b mirror plane). As we are interested here mainly in the dispersion of the low-energy transverse phonon branches, we shall consider that this 'longitudinal' coupling of easy rotations is infinitely strong. Then there are perfect correlations between each betaine and its nearest 'longitudinal' neighbour Ca complex. In this case the easy rotation of each betaine 1 entails simultaneously a corresponding rotation of the two nearest Ca complexes $2'$. The same holds for betaine 2 (3 and 4, respectively) and the nearest Ca complexes $4'$ ($1'$ and $3'$, respectively). Consequently, there remain only four independent rotational degrees of freedom in the unit cell, and thus only two (extended) phonon branches related to these correlated easy rotations. Obviously, following the original proposal of Dvořák [12] discussed above, these can be attributed to the two low-energy transverse optic branches observed in the experiment. Let us stress that these correlations associate entities belonging to *different* symmetrical formula units,

lying in *different* mirror planes σ_b. In fact, owing to the existence of these symmetry planes the correlated entities form infinite strands spreading along the *b* direction. In the following the sequences of strongly correlated betaine molecules and Ca complexes will be called '*columns*' (figure 2 and figure 3(a)). In figure 3(b) we represent each column by the projection of its axis of mass onto the *a–c* plane. It is convenient to label columns containing betaines 1 and Ca complexes 2′ by the letter A, and similarly columns containing betaines 2 (3 and 4, respectively) and Ca complexes 4′ (1′ and 3′, respectively) by the letter C (B and D, respectively). Different columns in each family are distinguished by the other two indices *h* and *l*, specifying the *x* and *z* coordinates of the unit cell to which a given column belongs.

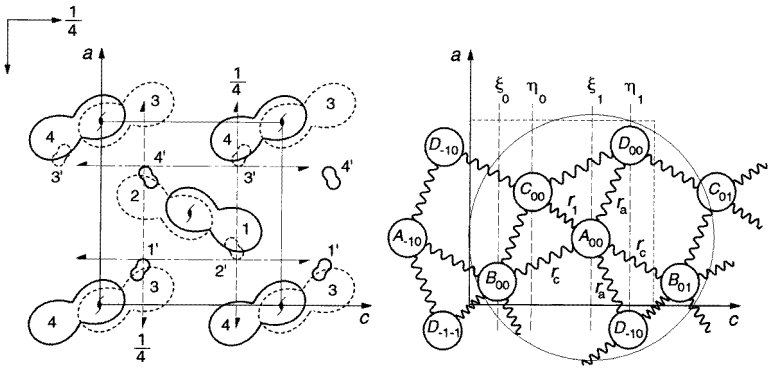

(a) (b)

Figure 3. Schematic representation of the crystal structure, projected onto the (*a–c*) plane. (a) Betaine molecules 1, 2, 3 and 4 and Ca complexes $1', 2', 3'$ and $4'$ are represented by the polar diagrams of their thermal librations. Units $1, 1', 4$ and $4'$ (full curve) are in the mirror plane σ_b at $y = \frac{1}{4}$, while the units $2, 2', 3$ and $3'$ (broken curve) belong to the mirror plane at $y = \frac{3}{4}$. Labels 1–4 are defined in the text (see section 2.2 and figure 2). (b) The 'columns'. The betaines and neighbouring inorganic Ca complexes are assembled in '*columns*'. As explained in the text, the 'easy displacements' of the entities belonging to the same column are strongly correlated. Consequently, they are described by only one collective variable for each *kind* of easy displacement, i.e. by one translational and one rotational variable. The symbols illustrate the notation adopted in sections 2.2 and 2.3. The circle centred on the axis of column A_{00} represents the 'interaction radius'. Direct coupling between variables defined on the column A_{00} and those defined on the columns outside this cylinder are neglected.

To each column we ascribe one 'column variable' ($\alpha_{h,l}$, $\beta_{h,l}$, $\gamma_{h,l}$ and $\delta_{h,l}$ for the columns $A_{h,l}$, $B_{h,l}$, $C_{h,l}$ and $D_{h,l}$, respectively). Each variable is understood as a mass-reduced amplitude of correlated easy rotations along the corresponding column and is considered as positive when the resulting dipole moment of the column is oriented in the positive sense of the *b* axis.

To describe the acoustic modes, the translational degrees of freedom are necessary. Following similar arguments to those given for the easy rotations, we introduce translational variables $a_{h,l}$, $b_{h,l}$, $c_{h,l}$ and $d_{h,l}$ describing mass-reduced translational amplitudes of the corresponding column as a whole in the *b* direction.

Because of the symmetry of the crystal, the variables introduced are mutually related by the symmetry operations of the Pnma space group, as seen in table 1 for the rotational variables ($\alpha_{h,l}$, $\beta_{h,l}$, $\gamma_{h,l}$ and $\delta_{h,l}$). Similar relations are obtained for the translational variables ($a_{h,l}$, $b_{h,l}$, $c_{h,l}$ and $d_{h,l}$).

Table 1. Symmetry properties for the 'rotational' variables.

	Rotational variables					
E	$\alpha_{h,l}$	$\beta_{h,l}$	$\gamma_{h,l}$	$\delta_{h,l}$	ξ_n	η_n
$\sigma_a(\frac{1}{2}\,\frac{1}{2}\,\frac{1}{2})$	$\beta_{-h,l+1}$	$\alpha_{-h,l}$	$\delta_{-h-1,l}$	$\gamma_{-h-1,l+1}$	ξ_{n+1}	η_{n+1}
$\sigma_c(\frac{1}{2}\,0\,\frac{1}{2})$	$\delta_{h,-l-1}$	$\gamma_{h,-l}$	$\beta_{h+1,-l}$	$\alpha_{h+1,-l-1}$	η_{-n}	ξ_{-n}
$\sigma_b(0\,\frac{1}{2}\,0)$	$-\alpha_{h,l}$	$-\beta_{h,l}$	$-\gamma_{h,l}$	$-\delta_{h,l}$	$-\xi_n$	$-\eta_n$

For the purpose of the analysis of the phonon dispersion along the Λ direction ($\boldsymbol{q} \parallel \boldsymbol{c}^*$) it is sufficient to introduce the displacement fields that depends on the index l only. In this case it is convenient to introduce new variables ξ_n and η_n for rotations and x_n and y_n for translations. They describe correlated displacements of whole layers of columns, perpendicular to the direction c.

From the symmetry relations, one sees that the index n takes the values $2l$ (for B and C) or $2l+1$ (for A and D). Namely, the glide plane n (σ_a) operates on x_n, y_n, ξ_n and η_n formally as translation operator with the halved period $c/2$. Therefore, the phonon eigenvectors may be defined only in one half of the unit cell, if the range of independent phonon wavevectors $\boldsymbol{q} \parallel \boldsymbol{c}^*$ is simultaneously extended twice, as if the true periodicity of the crystal were $c/2$. We shall see in the next paragraph that such a definition enables one to write the potential function in a very compact form.

Finally, for the analysis of the dispersion along the direction $\Sigma(\boldsymbol{q} \parallel \boldsymbol{a}^*)$ it is possible to introduce similar variables $\tilde{x}_m$, $\tilde{y}_m$, $\tilde{\xi}_m$ and $\tilde{\eta}_m$ that play the same role as those introduced earlier for $\boldsymbol{q} \parallel \boldsymbol{c}^*$.

2.3. Relevant interaction terms

Eight low-frequency dispersion curves in any direction $\boldsymbol{q} \perp \boldsymbol{b}^*$ (namely four extended Λ_3–Λ_2 and four extended Σ_4–Σ_2 branches) may be calculated from the quasi-harmonic part of the free energy expressed as a function of the variables introduced above. Such a free energy may be obtained from the total crystal potential after averaging out all non-relevant coordinates. The quasi-harmonic force constants corresponding to the coupling between two variables defined on any chosen couple of columns would then be given by the harmonic and anharmonic interactions between atoms belonging to two columns. We propose here to retain only some of the near-neighbour 'intercolumn' force constants as fitting parameters and to neglect totally the interaction between more distant columns.

For the translational variables we suggest considering only the coupling of each variable with those of the four neighbouring columns connected by deuterium bonds. For example, the variable a_{00} describing the translation of column A_{00} is then coupled to the variables d_{00}, $d_{-1,0}$, b_{00} and b_{01}. The corresponding contribution to the quasi-harmonic potential can be written in the form

$$\Delta F_t = \tfrac{1}{2}t_0 a_{00}^2 + t_a d_{00}a_{00} + t_a a_{00}d_{-1,0} + t_c a_{00}b_{00} + t_c a_{00}b_{01}$$

where t_a stands for the coupling constant for the pair of columns linked by deuterium bonds parallel to $\boldsymbol{a}$ (those related by σ_c) and t_c stands for the coupling constant for the pair of columns linked by deuterium bonds parallel to the $\boldsymbol{b}+\boldsymbol{c}$ and $\boldsymbol{b}-\boldsymbol{c}$ directions (those related by σ_a). The 'self'-coupling constant t_c is determined by the condition of translational

invariance:

$$t_0 = -2t_a - 2t_c$$

which ensures that an equal translation of all columns does not change the total energy.

For the coupling between rotational variables we suggest adding also the coupling between the two nearest-neighbour columns related by the C_{2b} operation. First, because it is the rotation of the betaine molecule that dominates in the rotational degree of freedom and the betaine molecules of the two nearest-neighbour columns related by C_{2b} are quite close to each other. Secondly, the rotational degrees of freedom create non-zero total column dipole moments p_y which certainly add important dipole–dipole Coulomb contributions to the rotation–rotation coupling constants. As such contributions depend on the intercolumn distance, a coherent approximation should account for all columns up to a certain distance. Including the interactions between the nearest-neighbour columns related by C_{2b}, σ_c and σ_a (r_1, r_a and r_c) corresponds to defining an 'interaction cylinder' with a diameter of about 15 Å (1.5 times the unit-cell parameter). The quasi-harmonic potential containing terms which couple the easy rotations inside column A_{00} with those of the neighbouring columns then reads

$$\Delta F_r = \tfrac{1}{2} r_0 \alpha_{00}^2 + r_1 \gamma_{00}\alpha_{00} + r_a \delta_{00}\alpha_{00} + r_a \alpha_{00}\delta_{-1,0} + r_c \alpha_{00}\beta_{00} + r_c \alpha_{00}\beta_{01}.$$

The self-coupling constant r_0 is here an independent parameter specifying the quasi-harmonic force constant describing the return torque acting on the easy rotations of a given column when displacements of all neighbouring columns are held fixed. Let us remark that from the microscopic point of view this coupling constant depends on both the intracolumn and the intercolumn atomic interactions.

Finally for the coupling between the translational and rotational variables we retain only the terms corresponding to the nearest-neighbour columns related by σ_c and σ_a. The variables a_{00} and α_{00} appear in the following translation–rotation coupling terms:

$$\Delta F_s = s_0\alpha_{00}a_{00} + s'_a\alpha_{00}d_{00} + s''_a\alpha_{00}d_{-1,0} + s''_c\alpha_{00}b_{00} + s'_c\alpha_{00}b_{01} + s''_a a_{00}\delta_{00} + s'_a a_{00}\delta_{-1,0} + s'_c a_{00}\beta_{00} + s''_c a_{00}\beta_{01}.$$

Note that the coupling constants for the interaction of column A with the two nearest-neighbour B columns (or D columns, respectively) are distinguished here as there is no symmetry relation between the translational and rotational displacements. Moreover, it might be expected that they are quite different or even of opposite signs, as the atoms on the different sides of the rotation axis of the rotating unit are displaced in opposite senses. The condition for the translational invariance provides

$$s_0 = -s'_a - s'_c - s''_a - s''_c.$$

The total quasi-harmonic potential in the present model is given by the sum of three types of coupling terms:

$$F = F_t + F_s + F_r$$

$$F_t = N_k \sum_{h,l} \{\tfrac{1}{2} t_0 (a_{hl}^2 + b_{hl}^2 + c_{hl}^2 + d_{hl}^2) + \cdots\}$$

$$F_s = N_k \sum_{h,l} \{s_0 (a_{hl}\alpha_{hl} + b_{hl}\beta_{hl} + c_{hl}\gamma_{hl} + d_{hl}\delta_{hl}) + \cdots\}$$

$$F_r = N_k \sum_{h,l} \{\tfrac{1}{2} r_0 (\alpha_{hl}^2 + \beta_{hl}^2 + \gamma_{hl}^2 + \delta_{hl}^2) + \cdots\}$$

$$N_k = \sum_k 1.$$

As all columns are symmetry related, each column has equivalent surroundings and there are only ten independent parameters (t_a, t_c, s'_a, s'_c, s''_a, s''_c, r_a, r_c, r_0 and r_1) in the potential. For the displacement fields that do not depend on the index h, this potential can be expressed in the variables x_n, y_n, ξ_n and η_n:

$$\begin{aligned}
F &= F_t + F_s + F_r \\
F_t &= N_{h,k} \sum_n \{\tfrac{1}{2} t_0 (x_n^2 + y_n^2) + 2t_a x_n y_n + t_c (x_n x_{n+1} + y_n y_{n+1})\} \\
F_s &= N_{h,k} \sum_n \{s_0 (\xi_n x_n + \eta_n y_n) + (s'_a + s''_a)(\xi_n y_n + \eta_n x_n) + s'_c (x_n \xi_{n+1} + \eta_n y_{n+1}) \\
&\quad + s''_c (x_{n+1} \xi_n + \eta_{n+1} y_n)\} \\
F_s &= N_{h,k} \sum_n \{\tfrac{1}{2} r_0 (\xi_n^2 + \eta_n^2) + r_1 \xi_{n+1} \eta_n + 2r_a \xi_n \eta_n + r_c (\xi_n \xi_{n+1} + \eta_n \eta_{n+1})\} \\
N_{h,k} &= \sum_{h,k} 1.
\end{aligned} \tag{2.1}$$

3. Lattice modes propagating along the c^* and a^* directions

Phonon frequencies corresponding to the 'easy displacements', as defined above, can be calculated as eigenvalues of the Fourier transformed force constant matrix of the proposed model potential. The resulting matrix may be viewed as a truncated submatrix of the full dynamical matrix of the crystal. However, in order to appreciate the role of the different coupling terms on the resulting phonon dispersions, it is useful to examine the structure of this truncated dynamical matrix itself (in the following called simply the 'dynamical matrix'). The discussion becomes particularly transparent for the case of dispersion along the principal symmetry directions a^* and c^*, provided that the dynamical matrix is given in a convenient symmetry basis.

3.1. The bare modes and the dynamical matrix

For the analysis of phonons propagating along c^*, such a basis may be formed by the following combinations, symmetric and antisymmetric with respect to the $\sigma_z(\frac{1}{2}\,0\,0)$ glide:

$$\phi_n = \frac{\xi_n + \eta_n}{\sqrt{2}} \qquad \psi_n = \frac{\xi_n - \eta_n}{\sqrt{2}} \qquad u_n = \frac{x_n + y_n}{\sqrt{2}} \qquad v_n = \frac{x_n - y_n}{\sqrt{2}}. \tag{3.1}$$

The symmetric variables ϕ_n and u_n have thus the same symmetry properties as the 'layer' variables w_n used in the articles of Chen and Walker [8] (and similarly the antisymmetric variables ψ_n and v_n transform as the v_n variables used therein). The spatial complex Fourier transforms (with halved translational period $\frac{1}{2}c$) of these variables

$$\begin{aligned}
\phi(q) &= \sum_n \phi_n \, \mathrm{e}^{(\mathrm{i}\pi q n)} \qquad & \psi(q) &= \sum_n \psi_n \, \mathrm{e}^{(\mathrm{i}\pi q n)} \\
u(q) &= \sum_n u_n \, \mathrm{e}^{(\mathrm{i}\pi q n)} \qquad & v(q) &= \sum_n v_n \, \mathrm{e}^{(\mathrm{i}\pi q n)}
\end{aligned} \tag{3.2}$$

may be interpreted as collective displacement coordinates with respect to the orthonormal basis of bare modes:

$$\{|\phi(q)\rangle, |\psi(q)\rangle, |u(q)\rangle, |v(q)\rangle\} \tag{3.3}$$

so that

$$\phi(q) \equiv \langle\phi(q)| \text{ any general displacement state } \rangle, \ldots \|\phi(q)\|^2 = \langle\phi(q)|\phi(q)\rangle = \sum_n 1 \equiv N_n, \ldots.$$

One may refer to these modes as to the bare or pure modes as they correspond to the displacements involving either only 'easy rotations' ($|\phi(q)\rangle$ and $|\psi(q)\rangle$) or only overall column translations T_y ($|u(q)\rangle$ and $|v(q)\rangle$).

They might be considered also as symmetry-adapted modes as they have all the transformation properties of the true 'eigenvector' phonon modes. Namely, all the four bare branches belong to the Λ_3 representation for $q \in \langle 0, \frac{1}{2}\rangle$ and they transform as Λ_2 modes with wavevectors $1 - q$ for $q \in \langle\frac{1}{2}, 1\rangle$. (The true crystallographic unit-cell parameter $c \approx 10.8$ Å is used here to define the reduced phonon wavevector $q = \boldsymbol{q} \cdot \boldsymbol{c}/2\pi$.) The symmetry of the bare Γ-point modes are as follows:

(i) $|\phi(0)\rangle$ and $|u(0)\rangle$ belong to the B_{2u} representation;
(ii) $|\psi(0)\rangle$ and $|v(0)\rangle$ belong to the B_{3g} representation;
(iii) $|\phi(1)\rangle$ and $|u(1)\rangle$ belong to the B_{1g} representation;
(iv) $|\psi(1)\rangle$ and $|v(1)\rangle$ belong to the A_u representation.

The corresponding dynamical matrix is obtained directly from the potential (2.1):

$$(D)_{X,Y} \equiv \frac{\langle X|D|Y\rangle}{N_n} = \sum_n \frac{1}{N_{h,k}} \frac{\partial^2 F}{\partial X_0 \, \partial Y_n} \mathrm{e}^{-\mathrm{i}\pi q n} \qquad X_n, Y_n = \phi_n, \psi_n, u_n, v_n \tag{3.4}$$

which leads to

$$D_c(q) = \begin{bmatrix} D_{vv} & 0 & D_{v\phi} & D_{v\psi} \\ 0 & D_{uu} & D_{u\phi} & D_{u\psi} \\ D^*_{v\phi} & D_{u\phi} & D_{\phi\phi} & D_{\phi\psi} \\ D_{v\psi} & D^*_{u\psi} & D^*_{\phi\psi} & D_{\psi\psi} \end{bmatrix} \tag{3.5}$$

where

$$\begin{aligned} D_{vv} &= A_a + A_c \sin^2\left(\frac{\pi q}{2}\right) \\ D_{uu} &= A_c \sin^2\left(\frac{\pi q}{2}\right) \\ D_{\phi\phi} &= b_{B_{2u}} + (b_{B_{1g}} - b_{B_{2u}}) \sin^2\left(\frac{\pi q}{2}\right) \\ D_{\psi\psi} &= b_{A_u} + (b_{B_{3g}} - b_{A_u}) \cos^2\left(\frac{\pi q}{2}\right) \\ D_{v\phi} &= \mathrm{i}d_c \sin(\pi q) \\ D_{v\psi} &= d_{B_{3g}} + d_{B_{1g}} \sin^2\left(\frac{\pi q}{2}\right) \\ D_{u\phi} &= d_{B_{1g}} \sin^2\left(\frac{\pi q}{2}\right) \\ D_{u\psi} &= \mathrm{i}d_c \sin(\pi q) \\ D_{\phi\psi} &= \mathrm{i}d_{12} \sin(\pi q) \end{aligned} \tag{3.6}$$

with ten real parameters (nine of them being independent):

$$\begin{aligned}
&A_c = -4t_c \\
&A_a = -4t_a \\
&b_{B_{2u}} = r_0 + r_1 + 2r_c + 2r_a \\
&b_{A_u} = r_0 + r_1 - 2r_c - 2r_a \\
&b_{B_{1g}} = r_0 - r_1 - 2r_c + 2r_a \\
&b_{B_{3g}} = r_0 - r_1 + 2r_c - 2r_a \\
&d_{12} = -r_1 = -(b_{B_{2u}} + b_{A_u} - b_{B_{1g}} - b_{B_{3g}})/4 \\
&d_{B_{1g}} = -2s_c' - 2s_c'' \\
&d_{B_{3g}} = -2s_a' - 2s_a'' \\
&d_c = s_c' - s_c''.
\end{aligned} \tag{3.7}$$

The diagonal elements of (3.5) correspond to the dispersion of the bare branches (consecutively $|v(q)\rangle$, $|u(q)\rangle$, $|\phi(q)\rangle$ and $|\psi(q)\rangle$); the non-diagonal elements are responsible for the eigenvector mixing. The parameters $b_{B_{2u}}$, b_{A_u}, $b_{B_{1g}}$ and $b_{B_{3g}}$ are the squared frequencies of the bare 'rotational' modes of B_{2u}, A_u, B_{1g} and B_{3g} symmetry; similarly A_c and A_a correspond to the bare translational modes B_{1g} and B_{3g}. Note that there is no direct coupling between the two bare translational branches, because the direct interaction between translations of the two nearest-neighbour columns related by the C_{2b} interaction was neglected, whereas the bare rotational branches are directly mixed by the $d_{12}\sin(\pi q)$ term.

One can proceed in a similar manner for the dispersion along the Σ line ($\boldsymbol{q} \parallel \boldsymbol{a}^*$). Let us introduce the extended bare Σ_4–Σ_2 branches in the following way:

$$\begin{aligned}
&\tilde{\phi}(q) = \sum_m \tilde{\phi}_m \,\mathrm{e}^{(\mathrm{i}\pi qm)} \qquad \tilde{\psi}(q) = \sum_m \tilde{\psi}_m \,\mathrm{e}^{(\mathrm{i}\pi qm)} \\
&\tilde{u}(q) = \sum_m \tilde{u}_m \,\mathrm{e}^{(\mathrm{i}\pi qm)} \qquad \tilde{v}(q) = \sum_m \tilde{v}_m \,\mathrm{e}^{(\mathrm{i}\pi qm)}
\end{aligned} \tag{3.8}$$

where the symmetric and antisymmetric combinations of the variables defined previously were introduced in the form

$$\tilde{\phi}_n = \frac{\tilde{\xi}_n + \tilde{\eta}_n}{\sqrt{2}} \qquad \tilde{\psi}_n = \frac{\tilde{\xi}_n - \tilde{\eta}_n}{\sqrt{2}} \qquad \tilde{u}_n = \frac{\tilde{x}_n + \tilde{y}_n}{\sqrt{2}} \qquad \tilde{v}_n = \frac{\tilde{x}_n - \tilde{y}_n}{\sqrt{2}} \tag{3.9}$$

so that

(i) $|\tilde{\phi}(0)\rangle = |\phi(0)\rangle$ and $|\tilde{u}(0)\rangle = |u(0)\rangle$ belong to the B_{2u} representation,
(ii) $|\tilde{\phi}(1)\rangle = |\psi(0)\rangle$ and $|\tilde{u}(1)\rangle = |v(0)\rangle$ belong to the B_{3g} representation,
(iii) $|\tilde{\psi}(0)\rangle = |\phi(1)\rangle$ and $|\tilde{v}(0)\rangle = |u(1\rangle$ belong to the B_{1g} representation and
(iv) $|\tilde{\psi}(1)\rangle = |\psi(1)\rangle$ and $|\tilde{v}(1)\rangle = |v(1)\rangle$ belong to the A_u representation.

The resulting dynamical matrix (for $\boldsymbol{q} \parallel \boldsymbol{a}^*$) is then the same as (3.5), but with elements

$$\begin{aligned}
D_{\tilde{v}\tilde{v}} &= A_c + A_a \sin^2\left(\frac{\pi q}{2}\right) \\
D_{\tilde{u}\tilde{u}} &= A_a \sin^2\left(\frac{\pi q}{2}\right) \\
D_{\tilde{\phi}\tilde{\phi}} &= b_{B_{2u}} + (b_{B_{3g}} - b_{B_{2u}}) \sin^2\left(\frac{\pi q}{2}\right) \\
D_{\tilde{\psi}\tilde{\psi}} &= b_{A_u} + (b_{B_{1g}} - b_{A_u}) \cos^2\left(\frac{\pi q}{2}\right) \\
D_{\tilde{v}\tilde{\phi}} &= \mathrm{i}d_a \sin(\pi q) \\
D_{\tilde{v}\tilde{\psi}} &= d_{B_{1g}} + d_{B_{3g}} \sin^2\left(\frac{\pi q}{2}\right) \\
D_{\tilde{u}\tilde{\phi}} &= d_{B_{3g}} \sin^2\left(\frac{\pi q}{2}\right) \\
D_{\tilde{u}\tilde{\psi}} &= \mathrm{i}d_a \sin(\pi q) \\
D_{\tilde{\phi}\tilde{\psi}} &= \mathrm{i}d_{12} \sin(\pi q).
\end{aligned} \tag{3.10}$$

The diagonal elements corespond, in that order, to the $\tilde{v}(q)$, $\tilde{u}(q)$, $\tilde{\phi}(q)$ and $\tilde{\psi}(q)$ bare branches. Here the parameter d_a is given by

$$d_a = s_a'' - s_a' \tag{3.11}$$

and the remaining parameters are defined as in (3.7).

3.2. The phonon eigenmodes

For a general value of $\boldsymbol{q} \parallel \boldsymbol{c}^*$ all the phonon eigenmodes (corresponding to the eigenvectors of the dynamical matrix) are of mixed character. However, in the $q \to 0$ limit, most of the mixing terms disappear and only the $d_{B_{3g}}$ term which couples the two bare B_{3g} modes $|\psi(0)\rangle$ and $|v(0)\rangle$ will remain. Similarly, for $q = 1$, only the mixing between the two B_{1g} modes ($|\phi(1)\rangle$ and $|u(1)\rangle$ coupled by $d_{B_{1g}}$) and between the two A_u modes ($|\psi(1)\rangle$ and $|v(1)\rangle$ coupled by $d_{A_u} = d_{B_{1g}} + d_{B_{3g}}$) remain. Consequently, the Γ-point eigenmodes fulfil the following conditions:

$$\omega_{B_{2u}} = \omega^2_{B_{2u}(L)} = b_{B_{2u}} \tag{3.12}$$

and

$$\begin{aligned}
\omega^2_{B_{1g}(L)} + \omega^2_{B_{1g}(T)} &= A_c + b_{B_{1g}} \\
\omega^2_{B_{1g}(L)}\omega^2_{B_{1g}(T)} &= A_c b_{B_{1g}} - d^2_{B_{1g}} \\
\omega^2_{B_{3g}(L)} + \omega^2_{B_{3g}(T)} &= A_a + b_{B_{3g}} \\
\omega^2_{B_{3g}(L)}\omega^2_{B_{3g}(T)} &= A_a b_{B_{3g}} - d^2_{B_{3g}} \\
\omega^2_{A_u(L)} + \omega^2_{A_u(T)} &= A_a + b_{A_u} + A_c \\
\omega^2_{A_u(L)}\omega^2_{A_u(T)} &= (A_a + A_c) b_{A_u} - d^2_{A_u}
\end{aligned} \tag{3.13}$$

where the additional index T (or L) distinguishes the eigenmodes which become bare translational (or librational) modes when the non-diagonal terms are continuously switched off. If these mixing terms $d_{B_{1g}}$, $d_{B_{3g}}$ and d_{A_u} are small enough with respect to the difference of the squared frequencies of the corresponding bare modes, the eigenvectors of the resulting modes keep approximately their original character. We suppose that this is indeed the case, because the similar characteristics of the lowest B_{1g}, B_{3g} and A_u optic phonons

(established experimentally; see part I) suggest that their eigenvectors correspond to the 'critical' librational degrees of freedom.

Once these lowest-frequency modes are identified with the $B_{1g}(L)$, $B_{3g}(L)$ and $A_u(L)$ eigenmodes, the optic phonons with dominant translational eigenvectors $B_{1g}(T)$, $B_{3g}(T)$ and $A_u(T)$ must have higher frequencies. Under these conditions more explicit estimates for the Γ-point eigenvalues of the dynamical matrix can be derived as

$$\begin{aligned}
\omega^2_{B_{1g}(L)} &= b_{B_{1g}} - \frac{d^2_{B_{1g}}}{A_c - b_{B_{1g}}} + (A_c - b_{B_{1g}})\mathcal{O}\left[\left(\frac{d_{B_{1g}}}{(A_c - b_{B_{1g}}}\right)^4\right] \\
\omega^2_{B_{1g}(T)} &= A_c + \frac{d^2_{B_{1g}}}{A_c - b_{B_{1g}}} + (A_c - b_{B_{1g}})\mathcal{O}\left[\left(\frac{d_{B_{1g}}}{(A_c - b_{B_{1g}}}\right)^4\right] \\
\omega^2_{B_{3g}(L)} &= b_{B_{3g}} - \frac{d^2_{B_{3g}}}{A_a - b_{B_{3g}}} + (A_a - b_{B_{3g}})\mathcal{O}\left[\left(\frac{d_{B_{3g}}}{(A_a - b_{B_{3g}}}\right)^4\right] \\
\omega^2_{B_{3g}(T)} &= A_a + \frac{d^2_{B_{3g}}}{A_a - b_{B_{3g}}} + (A_a - b_{B_{3g}})\mathcal{O}\left[\left(\frac{d_{B_{3g}}}{(A_a - b_{B_{3g}}}\right)^4\right] \\
\omega^2_{A_u(L)} &= c - \frac{d^2_{A_u}}{A_a - b_{A_u} + A_c} + (A_a - b_{A_u} + A_c)\mathcal{O}\left[\left(\frac{d_{A_u}}{(A_a - b_{A_u} + A_c}\right)^4\right] \\
\omega^2_{A_u(T)} &= A_a + A_c + \frac{d^2_{A_u}}{A_a - b_{A_u} + A_c} + (A_a - b_{A_u} + A_c)\mathcal{O}\left[\left(\frac{d_{A_u}}{(A_a - b_{A_u} + A_c}\right)^4\right]
\end{aligned} \tag{3.14}$$

where the three mixing elements are related by

$$d_{A_u} = d_{B_{1g}} + d_{B_{3g}}.$$

For the phonon modes with wavevectors in the vicinity of the Γ point, the dispersion of the eigenmodes can be obtained by a standard perturbation expansion with respect to the small parameter q (or $1 - q$). Here only the correction to the acoustic velocity due to the coupling of the acoustic branch with the optic branches is of practical interest. For $\boldsymbol{q} \parallel \boldsymbol{c}^*$, we obtain

$$\omega^2_{TA}(q) = [A_c - 4d_c^2 A_a(\omega^2_{B_{3g}(L)}\omega^2_{B_{3g}(T)})^{-1}]\left(\frac{\pi q}{2}\right)^2 + \mathcal{O}(q^3) \tag{3.15}$$

and, for $\boldsymbol{q} \parallel \boldsymbol{a}^*$;

$$\omega^2_{TA}(q) = [A_a - 4d_a^2 A_c(\omega^2_{B_{1g}(L)}\omega^2_{B_{1g}(T)})^{-1}]\left(\frac{\pi q}{2}\right)^2 + \mathcal{O}(q^3). \tag{3.16}$$

The elastic constants may thus be expressed as:

$$C_{44} = \rho[A_c - 4d_c^2 A_a(\omega^2_{B_{3g}(L)}\omega^2_{B_{3g}(T)})^{-1}]\left(\frac{\pi}{2}\right)^2 \tag{3.17}$$

and

$$C_{66} = \rho[A_a - 4d_a^2 A_c(\omega^2_{B_{1g}(L)}\omega^2_{B_{1g}(T)})^{-1}]\left(\frac{\pi}{2}\right)^2 \tag{3.18}$$

where ρ is the mass density of the crystal.

These expressions allow us to estimate the frequencies of the translational optic modes $\omega_{B_{3g}(T)}$, $\omega_{B_{1g}(T)}$ and $\omega_{A_u(T)}$ using the values of the elastic constants only:

$$\omega^2_{B_{1g}(T)} \overset{(3.14)}{\geqslant} A_c \overset{(3.17)}{\geqslant} C_{44}/\rho \qquad \omega^2_{B_{3g}(T)} \overset{(3.14)}{\geqslant} A_c \overset{(3.18)}{\geqslant} C_{66}/\rho. \tag{3.19}$$

In other words, the second mixed mode of mainly translational character has a higher frequency $\omega^2_{B_{1g}(T)}$ than the pure T_y mode (A_c) which is higher than the frequency extrapolated from the acoustic velocity.

In BCCD these relations provide the following inequalities:

$$\nu^2_{B_{1g}(T)} \overset{(3.19)}{\geqslant} 1.18\ \text{THz} \qquad \nu^2_{B_{3g}(T)} \overset{(3.19)}{\geqslant} 0.89\ \text{THz} \tag{3.20}$$

which allow us to identify the second-lowest-frequency phonons of the B_{1g} and B_{3g} representation (around 1.3 THz) as $B_{1g}(T)$ and $B_{3g}(T)$ (the next B_{1g} and B_{3g} modes are around 1.85 and 2.1 THz, respectively). Obviously, the smaller the coupling between translations and easy rotations, the closer the frequencies and corresponding estimates should be. If at least the $d^2_{B_{1g}}/(A_c - b_{B_{1g}})$, $d^2_{B_{3g}}/(A_a - b_{B_{3g}})$ and $d^2_{A_u}/(A_a - b_{A_u} + A_c)$ are small, the frequencies of the $\omega_{B_{3g}(T)}$, $\omega_{B_{1g}(T)}$ and $\omega_{A_u(T)}$ modes are approximately given by the corresponding bare modes and from (3.19) it further follows that

$$\nu^2_{A_u(T)} \doteq \nu^2_{B_{1g}(T)} + \nu^2_{B_{3g}(T)} \tag{3.21}$$

which provides the rough estimate

$$\nu_{A_u(T)} \approx 1.85\ \text{THz}.$$

We have indeed observed two modes with frequencies close to this value (at 1.6 and 1.85 THz) that may correspond to the A_u representation (see part I). It seems probable that only the mode at 1.85 THz is the A_u mode, which would support its interpretation as $A_u(T)$. However, in order not to include unnecessary uncertainties in the model, for the time being we shall leave the question of the assignment of this mode open.

The analysis of the dispersion inside the Brillouin zone is more complex, as all the mixing terms have to be considered simultaneously. This is particularly important in the region where the two bare optic branches cross the bare acoustic branch $u(q)$. Moreover, the resulting dispersions depend not only on the moduli of the mixing terms but also on their signs (unlike in the case of coupling between only two modes, as for example in (3.13)).

4. Comparison with the experimental dispersion

The qualitative considerations in the preceding sections lead us to propose a parametrization of the dynamical matrix in terms of ten independent parameters: A_c, A_a, $b_{B_{1g}}$, $b_{B_{3g}}$, $b_{B_{2u}}$, b_{A_u}, $d_{B_{1g}}$, $d_{B_{3g}}$, d_c and d_a. If this approach is essentially correct, each of these parameters should have a well defined physical interpretation. In particular, knowledge of their values enables one

(i) to trace the dispersion of the bare modes, the mixing terms and the eigenmodes along any general direction in the $\boldsymbol{a}^*$–$\boldsymbol{c}^*$ plane,

(ii) to express the eigenvectors of the eigenmodes as linear combinations of bare mode 'eigenvectors' and

(iii) to estimate the values of the ten mass-reduced intercolumn force constants t_c, t_a,

r_0, r_1, r_a, r_c, s'_c, s'_a, s''_c and s''_a, as (3.7) and (3.11) allow direct inversion:

$$\begin{aligned} t_c &= -\tfrac{1}{4}A_c \\ t_a &= -\tfrac{1}{4}A_a \end{aligned}$$

$$\begin{aligned} r_c &= \tfrac{1}{8}(b_{B_{2u}} - b_{A_u} - b_{B_{1g}} + b_{B_{3g}}) \\ r_a &= \tfrac{1}{8}(b_{B_{2u}} - b_{A_u} + b_{B_{1g}} - b_{B_{3g}}) \\ r_1 &= \tfrac{1}{4}(b_{B_{2u}} + b_{A_u} - b_{B_{1g}} - b_{B_{3g}}) = -d_{12} \\ r_0 &= \tfrac{1}{4}(b_{B_{2u}} + b_{A_u} + b_{B_{1g}} + b_{B_{3g}}) \end{aligned} \tag{4.1}$$

$$\begin{aligned} s'_c &= -\tfrac{1}{4}(d_{B_{1g}} - 2d_c) \\ s'_a &= -\tfrac{1}{4}(d_{B_{3g}} + 2d_a) \\ s''_c &= -\tfrac{1}{4}(d_{B_{1g}} + 2d_c) \\ s''_a &= -\tfrac{1}{4}(d_{B_{3g}} - 2d_a). \end{aligned}$$

In this section the determination of these parameters from the comparison with the experimental data is discussed.

As the potential introduced in section 2.3 was written directly in terms of mass-reduced variables, the above parameters correspond to mass-reduced force constants. In order to facilitate the comparison with the inelastic neutron scattering data presented in part I, we shall suppose that all introduced parameters are expressed in units of $4\pi^2$ THz^2 (10^{24} rad^2 s^{-2}).

4.1. Fitting procedure

The inverse lattice dynamics problem (setting up the free parameters in the dynamical matrix using the known dispersion curves) is not a straightforward procedure, because for example the different sets of free parameters in the dynamical matrix may provide the same or similar dispersion curves. Therefore, any simple approach such as the least-squares fit of the data with the eigenvalues of the parametrized dynamical matrix using arbitrarily chosen starting parameters is clearly insufficient, and a more systematic analysis is required.

Here we take advantage of the following four facts.

(i) Equations (3.12), (3.13), (3.17) and (3.18), the experimental zone centre frequency values of the modes $B_{2u}(L)$, $B_{1g}(L)$, $B_{3g}(L)$, $A_u(L)$, $B_{1g}(T)$, $B_{3g}(T)$ and the elastic constants C_{44} and C_{66} provide altogether eight independent constraints on the values of the ten model parameters. These constraints are unfortunately non-linear but, if the values of A_a and A_c and the signs of $d_{B_{1g}}$, $d_{B_{3g}}$, d_a and d_c are known, the eight remaining parameters $b_{B_{1g}}$, $b_{B_{3g}}$, $b_{B_{2u}}$, b_{A_u}, $d_{B_{1g}}$, $d_{B_{3g}}$, d_a and d_c can be evaluated explicitly from these conditions.

(ii) The upper and lower limits for A_a and A_c (describing the dispersion of the bare acoustic modes with $\boldsymbol{q} \parallel \boldsymbol{c}^*$ and $\boldsymbol{q} \parallel \boldsymbol{a}^*$) can be easily extracted from (3.14)–(3.16):

$$A_c \in \left\langle \frac{C_{44}}{\rho}\frac{4}{\pi^2}, \omega^2_{B_{1g}} \right\rangle \approx \langle 1.5, 1.9 \rangle \tag{4.2}$$

$$A_a \in \left\langle \frac{C_{66}}{\rho}\frac{4}{\pi^2}, \omega^2_{B_{3g}} \right\rangle \approx \langle 0.8, 1.6 \rangle. \tag{4.3}$$

(iii) The dispersion along c^* does not depend on the value and sign of d_a.

(iv) The eigenvalues of the matrix $D_c(q)$ do not change if the signs of the parameters $d_{B_{1g}}$, $d_{B_{3g}}$ and d_c are changed simultaneously; this follows from the fact that $d_{B_{1g}}$, $d_{B_{3g}}$ and d_c appear as pair products in the characteristic polynomial of $D_c(q)$ ($p(\lambda) = \det|D_c(q) - \lambda\mathcal{I}|$).

The fitting procedure itself was as follows.

(1) The signs of $d_{B_{1g}}$, $d_{B_{3g}}$ and d_c were chosen.

(2) A trial value of A_c was chosen within the allowed interval (4.2).

(3) Using (3.12), (3.13), (3.17) and (3.18), the values of the remaining parameters and the smallest eigenvalue of the matrix $D_c(\frac{1}{3})$ were calculated as a function A_a, for $A_a \in \langle 0.8, 1.6\rangle$ (see (4.3)).

(4) For those values of A_a for which the calculated lowest eigenvalue at $q = \frac{1}{3}$ corresponded to the square of the experimental soft-mode frequency, all dispersion curves along c^* were calculated and compared with the experimental data.

(5) In the case of reasonable agreement with the dispersion curves along c^*, the dispersion curves along a^* were calculated as well (once with d_a negative and once with d_a positive).

(6) Points (2)–(5) were repeated for different values of the parameter A_c in the allowed interval (4.2).

(7) Points (1)–(6) were repeated for all four non-equivalent sign choices for $d_{B_{1g}}$, $d_{B_{3g}}$ and d_c ($(+++)$, $(++-)$, $(+--)$ and $(+-+)$).

4.2. Results

The above-described procedure was applied first to the data collected at 205 K, which are quite complete and which already reveal the well developed minimum on the lowest phonon branch. Two different sets of parameters providing very satisfactory fits for the dispersion along c^* were found. The first variant corresponds to the $(++++)$ choice ($d_{B_{1g}} > 0$, $d_{B_{3g}} > 0$, $d_c > 0$, $d_a > 0$); the second variant corresponds to the $(-+++)$ choice (see figures 4 and 5 and tables 2 and 3).

In both cases a minimum on the soft branch appears owing to the simultaneous mixing between the acoustic branch and both 'rotational' optic branches. This can be easily verified by changing the sign of one of the three mixing terms involved. If there were only pair mixing, this change would have no effect on the dispersion, because pair mixing gives rise to a mode repulsion which depends on the modulus of the mixing term. On the contrary we observe quite drastic changes, leading to the disappearance of the minimum on the Λ_3 branch and the appearance of a minimum or even an instability on the Σ_4 branch (figure 6).

The simultaneous mixing of all three branches allows also a better understanding of the difference between dispersions for $\boldsymbol{q} \parallel \boldsymbol{c}^*$ and $\boldsymbol{q} \parallel \boldsymbol{a}^*$. If the mixing of branches involved at each q only two branches at maximum, rather similar dispersions for both directions are predicted by the model. Indeed, in both cases the dispersion of the bare optic branches and of the bare acoustic branch are quite similar and the terms responsible for the mixing of easy rotations with the translations are of the same order, too.

The latter follows directly from the assumption of pair mixing, as the experimentally established anticrossing gaps in the regions where the bare branches cross are of same order of magnitude in both directions.

On the contrary, if the mixing is extended to all three branches, the repulsion of the lowest branch by the other two may be either additive or may partially cancel, according to the relative signs of the mixing terms, which may be different for the two directions.

Table 2. Values of the parameters that appear in the dynamical matrices (3.5) and (3.10), as deduced from the experimental mode frequencies.

	A_c ($4\pi^2$ THz^2)	A_a ($4\pi^2$ THz^2)	$b_{B_{2u}}$ ($4\pi^2$ THz^2)	$b_{B_{1g}}$ ($4\pi^2$ THz^2)	$b_{B_{3g}}$ ($4\pi^2$ THz^2)	b_{A_u} ($4\pi^2$ THz^2)	$d_{B_{1g}}$ ($4\pi^2$ THz^2)	$d_{B_{3g}}$ ($4\pi^2$ THz^2)	d_c ($4\pi^2$ THz^2)	d_a ($4\pi^2$ THz^2)
205 K first variant	1.89	1.5	0.13	0.497	0.54	0.228	0.240	0.423	0.238	0.306
205 K second variant	1.90	1.66	0.13	0.487	0.385	0.100	−0.208	0.080	0.229	0.333
300 K first variant	1.75	1.35	0.26	0.630	0.660	0.368	0.330	0.435	0.247	0.303

Table 3. Values of the quasi-harmonic intercolumn force constants, as obtained from the parameter values in table 2.

	t_c ($4\pi^2$ THz^2)	t_a ($4\pi^2$ THz^2)	r_0 ($4\pi^2$ THz^2)	r_1 ($4\pi^2$ THz^2)	r_a ($4\pi^2$ THz^2)	r_c ($4\pi^2$ THz^2)	s_c'' ($4\pi^2$ THz^2)	s_c' ($4\pi^2$ THz^2)	s_a' ($4\pi^2$ THz^2)	s_a'' ($4\pi^2$ THz^2)
205 K first variant	−0.473	−0.375	0.349	−0.170	−0.018	−0.007	−0.179	0.059	−0.259	0.047
205 K second variant	−0.475	−0.414	0.275	−0.161	0.017	−0.009	−0.062	0.166	−0.186	0.146
300 K first variant	−0.438	−0.338	0.475	−0.171	−0.015	−0.007	−0.206	0.041	−0.260	0.043

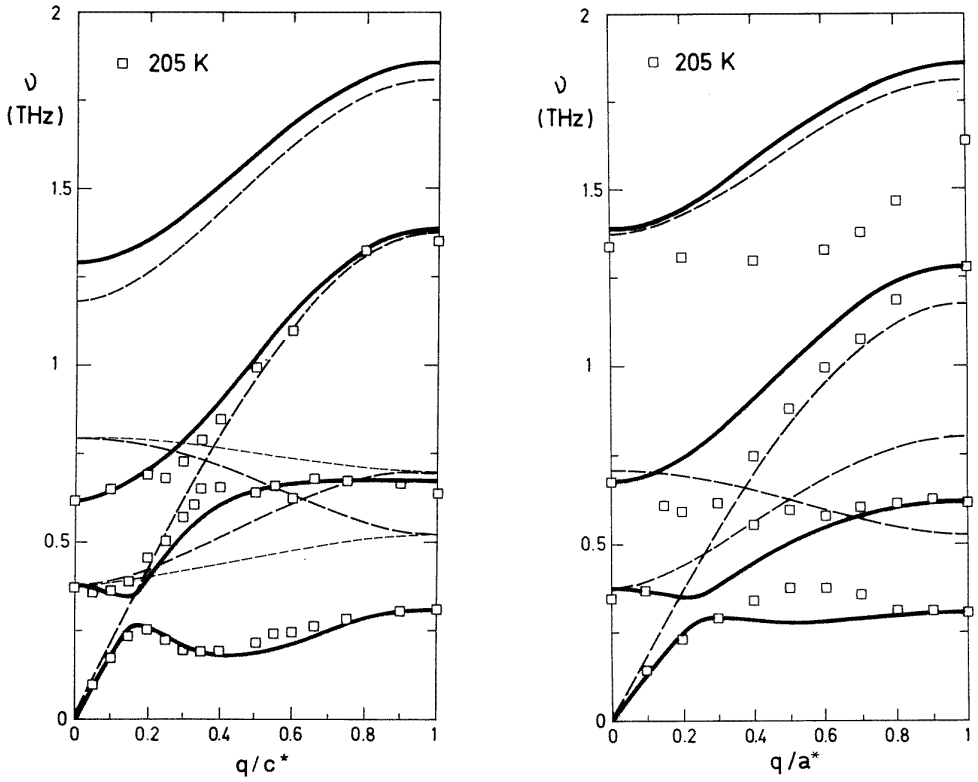

(a) (b)

Figure 4. Dispersion curves along the $\boldsymbol{a}^*$ and $\boldsymbol{c}^*$ directions at 205 K. The neutron data (see part I) are shown as open symbols. Solid curves represent dispersion curves of eigenmodes, and broken curves those of bare modes, calculated from the dynamical matrixes $D_c(q)$ and $D_a(q)$ for parameter values determined by the method described in the text (first variant, with $d_{B_{1g}} > 0$, $d_{B_{3g}} > 0$, $d_c > 0$, $d_a > 0$). (a) Dispersion for $\boldsymbol{q} \parallel \boldsymbol{c}^*$. The broken curve (— — —) represent the dispersion of the diagonal elements of the matrix $D_c(q)$, defined in section 3.7, while broken curves (– – –) represent the dispersion of the alternative 'flat' bare optic branches $D_{\phi'\phi'}$ and $D_{\psi'\psi'}$ (4.10), introduced in section 4.4. (b) Dispersion for $\boldsymbol{q} \parallel \boldsymbol{a}^*$. (c) Dispersion for $\boldsymbol{q} \parallel \boldsymbol{a}^*$, with the same set of parameters except for d_{12}, which was set to zero.

On the other hand, the difference between the two variants proposed does not allow one to be favoured over the other, because in both cases the observed discrepancies may possibly be accounted for by neglected interactions. In particular, small discrepancies should arise owing to the neglected dipole–dipole coupling between easy rotations of the more distant columns. For example, if the interaction between the next-neighbour columns related by C_{2y} are taken into account , the coupling constant d_{12} becomes an independent parameter, which may take on different values for the $D_c(q)$ and $D_a(q)$ dynamical matrices. We have found that setting $d_{12} = 0$ in the $D_a(q)$ matrix improves considerably the agreement with the experimental data (for $\boldsymbol{q} \parallel \boldsymbol{a}^*$, see figures 4 and 5), which is consistent with such a hypothesis. Therefore, the values of the parameters cannot be determined in a unique way by comparison with the experimental dispersions

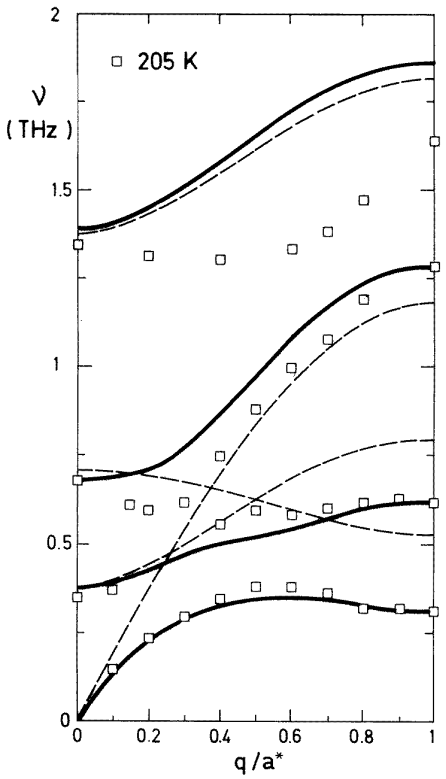

(c)

Figure 4. (Continued)

only.

The same procedure was applied also to the room-temperature data, with similar results (figure 7). The differences between parameter values at $T = 300$ and 200 K should in principle indicate which interactions have large anharmonic contributions. However, this method appears to be unreliable owing to the accumulation of experimental errors and uncertainties inherent in the fitting procedure. Instead, we limit our analysis to the temperature derivatives of the parameters, which may be estimated by a more direct and more reliable method discussed in the next section.

In the semimicroscopic approach, the effect of the anharmonicity is hidden in the temperature dependence of the quasi-harmonic force constants. The purpose of this section is to determine firstly which of the force constants has a temperature dependence that is essential for the observed soft-mode behaviour and secondly what kind of anharmonic interaction term is responsible for this renormalization.

4.3. The essential soft quasi-harmonic parameter

In order to find the quasi-harmonic force constant parameter which provides the main contribution to the observed decrease in the soft-mode frequency, let us consider the possible role of each of the coupling parameters one by one.

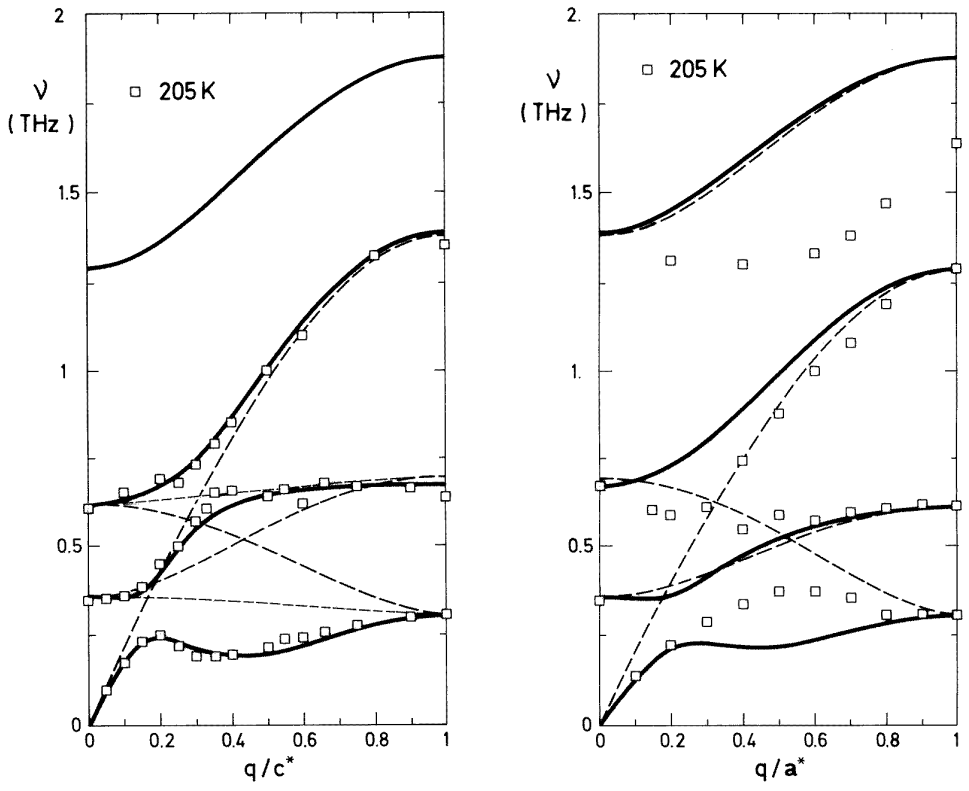

Figure 5. Dispersion curves along the $\boldsymbol{a}^*$ and $\boldsymbol{c}^*$ directions at 205 K for the second variant. The meaning of the symbols is same as in the preceding figure 4. The solid and broken curves are calculated from the parameter values determined by the method described in the text (second variant, with $d_{B_{1g}} < 0$, $d_{B_{3g}} > 0$, $d_c > 0$, $d_a > 0$). (a) Dispersion for $\boldsymbol{q} \parallel \boldsymbol{c}^*$. (b) Dispersion for $\boldsymbol{q} \parallel \boldsymbol{a}^*$. (c) Dispersion for $\boldsymbol{q} \parallel \boldsymbol{a}^*$, with the same set of parameters except for d_{12}, which was set to zero.

First of all, we may exclude the parameters t_a and t_c, as the bare acoustic modes show rather ordinary hardening with decreasing temperature. This is apparent both for the $B_{1g}(T)$ and the $B_{3g}(T)$ optic modes (which correspond roughly to the $q = 1$ end of the extended bare acoustic branches $u(q)$ and $u(\tilde{q})$) and also for the temperature dependence of the elastic constants C_{44} and C_{66} reported in [24].

The renormalization of the coupling constants s'_a, s'_c, s''_a and s''_c, describing the translation–rotation coupling, may in principle contribute to the soft-mode renormalization as was recently proposed in the case of K_2SeO_4 [25]. However, the temperature derivative of the $\omega^2_{B_{2u}(L)}$ frequency, which does not depend on the parameters s_i and t_i at all, is even higher than that of the soft mode itself. As it seems plausible that the temperature renormalization of the soft mode has the same origin as the renormalization of the lowest-energy zone centre modes $B_{1g}(L)$, $B_{3g}(L)$, $B_{2u}(L)$ and $A_u(L)$, the anharmonicity of the translation–rotation coupling is not a primary contribution.

Hence, the critical coupling constant is to be found among the force constants r_0, r_1, r_a and r_c. For this purpose it is useful to examine expressions for the squared frequencies

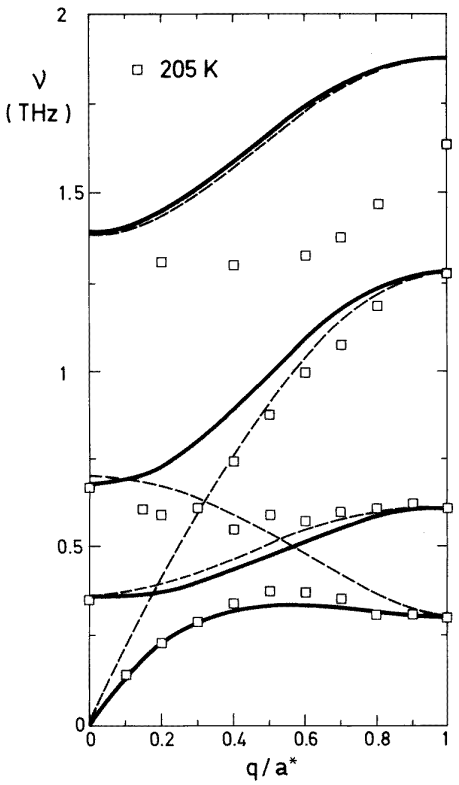

(c)

Figure 5. (Continued)

of the four Γ-point bare optic modes corresponding to the easy rotations in terms of the intercolumn force constants (see (3.7)):

$$\begin{aligned} b_{B_{2u}} &= r_0 + r_1 + 2r_c + 2r_a (\text{for the bare } B_{2u}) \\ b_{A_u} &= r_0 + r_1 - 2r_c - 2r_a \ (\text{for the bare } A_u) \\ b_{B_{1g}} &= r_0 - r_1 - 2r_c + 2r_a (\text{for the bare } B_{1g}) \\ b_{B_{3g}} &= r_0 - r_1 + 2r_c - 2r_a (\text{for the bare } B_{3g}). \end{aligned} \tag{4.4}$$

The only force constant that contributes to all these modes with the same sign is r_0; all others would soften some modes but simultaneously harden others. We may thus conclude that the parameter which contributes most to the softening of the two bare optic branches and indirectly to the soft-mode renormalization should be r_0.

As already mentioned, the r_0 'self'-coupling constant contains the contributions from both the intercolumn and the intracolumn interatomic force constants. Therefore, if the former were responsible for the temperature dependence of r_0, this temperature dependence should be observed simultanously for some other, purely intercolumn force constant parameter $r_i, i \neq 0$. Such a hypothesis can be rejected on the basis of the following qualitative analysis. First, we have the exact relation (3.12):

$$\frac{\partial}{\partial T}\omega^2_{B_{2u}(L)} = \frac{\partial}{\partial T} b_{B_{2u}}.$$

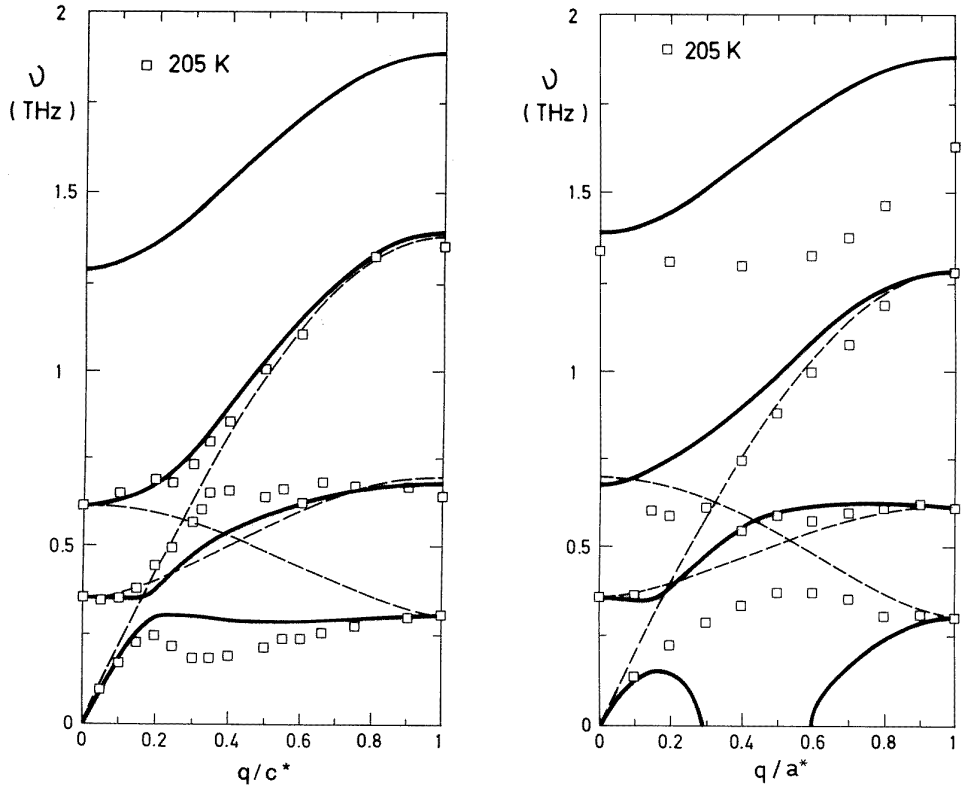

(a) (b)

Figure 6. The effect of the signs of the mixing terms. The neutron data (see part I) are shown as open symbols. The solid curves represent dispersion curves of eigenmodes, and the broken curves those of bare modes, calculated from the dynamical matrices $D_c(q)$ and $D_a(q)$ from the parameter values determined by the method described in the text (second variant). (a) Dispersion curves for $\boldsymbol{q} \parallel \boldsymbol{c}^*$ for the same set of parameter values as in figure 5, but with $d_c < 0$. (b) Dispersion curves for $\boldsymbol{q} \parallel \boldsymbol{a}^*$ for the same set of parameter values as in figure 5, but with $d_a > 0$.

If the temperature dependences of the parameters $d_{B_{1g}}$, $d_{B_{3g}}$ and d_{A_u} are neglected, it follows from (3.14) that the temperature derivatives of the squared frequencies of the $B_{1g}(L)$, $B_{3g}(L)$ and $A_u(L)$ eigenmodes may be approximated by the temperature derivatives of the squared frequencies of the bare 'rotational' modes:

$$\frac{\partial}{\partial T}\omega^2_{B_{1g}(L)} \doteq \frac{\partial}{\partial T} b_{B_{1g}} \qquad \frac{\partial}{\partial T}\omega^2_{B_{3g}(L)} \doteq \frac{\partial}{\partial T} b_{B_{3g}} \qquad \frac{\partial}{\partial T}\omega^2_{A_u(L)} \doteq \frac{\partial}{\partial T} b_{A_u}. \tag{4.5}$$

Then the temperature derivatives of the purely 'easy rotational' parameters 'r_i' can be

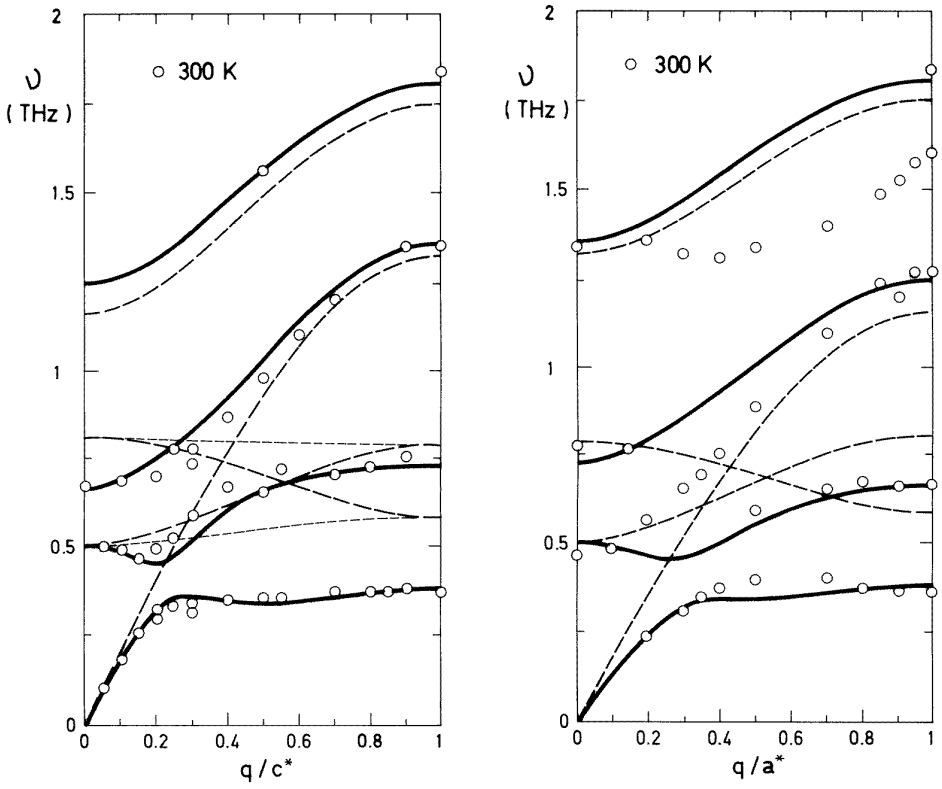

Figure 7. Dispersion curves along the $\boldsymbol{a}^*$ and $\boldsymbol{c}^*$ directions at 300 K. The neutron data (those of part I) are shown as by open circles. The solid curves represent dispersion curves of eigenmodes and the broken curves those of bare modes, calculated from the dynamical matrices $D_c(q)$ and $D_a(q)$ for parameter values determined by the method described in the text (first variant, with $d_{B_{1g}} > 0, d_{B_{3g}} > 0$, $d_c > 0$, $d_a > 0$). (a) Dispersion for $\boldsymbol{q} \parallel \boldsymbol{c}^*$. The broken curves (— — —) represent the dispersion of the diagonal elements of the matrix $D_c(q)$, defined in section 3.7, while the broken curves (– – –) represent the dispersion of the alternative 'flat' bare optic branches $D_{\phi'\phi'}$ and $D_{\psi'\psi'}$ (4.10), introduced in section 4.4. (b) Dispersion for $\boldsymbol{q} \parallel \boldsymbol{a}^*$. (c) Dispersion for $\boldsymbol{q} \parallel \boldsymbol{a}^*$, with the same set of parameters except for d_{12}, which was set to zero.

determined explicitly from

$$\begin{aligned}
\frac{\partial}{\partial T} r_c &\doteq \frac{1}{8}\left(\frac{\partial}{\partial T}\omega^2_{B_{2u}(L)} - \frac{\partial}{\partial T}\omega^2_{A_u(L)} - \frac{\partial}{\partial T}\omega^2_{B_{1g}(L)} + \frac{\partial}{\partial T}\omega^2_{B_{3g}(L)}\right) \\
\frac{\partial}{\partial T} r_a &\doteq \frac{1}{8}\left(\frac{\partial}{\partial T}\omega^2_{B_{2u}(L)} - \frac{\partial}{\partial T}\omega^2_{A_u(L)} + \frac{\partial}{\partial T}\omega^2_{B_{1g}(L)} - \frac{\partial}{\partial T}\omega^2_{B_{3g}(L)}\right) \\
\frac{\partial}{\partial T} r_1 &\doteq \frac{1}{4}\left(\frac{\partial}{\partial T}\omega^2_{B_{2u}(L)} + \frac{\partial}{\partial T}\omega^2_{A_u(L)} - \frac{\partial}{\partial T}\omega^2_{B_{1g}(L)} - \frac{\partial}{\partial T}\omega^2_{B_{3g}(L)}\right) \\
\frac{\partial}{\partial T} r_0 &\doteq \frac{1}{4}\left(\frac{\partial}{\partial T}\omega^2_{B_{2u}(L)} + \frac{\partial}{\partial T}\omega^2_{A_u(L)} + \frac{\partial}{\partial T}\omega^2_{B_{1g}(L)} + \frac{\partial}{\partial T}\omega^2_{B_{3g}(L)}\right).
\end{aligned} \tag{4.6}$$

Taking the experimental values of the temperature derivatives of the squared

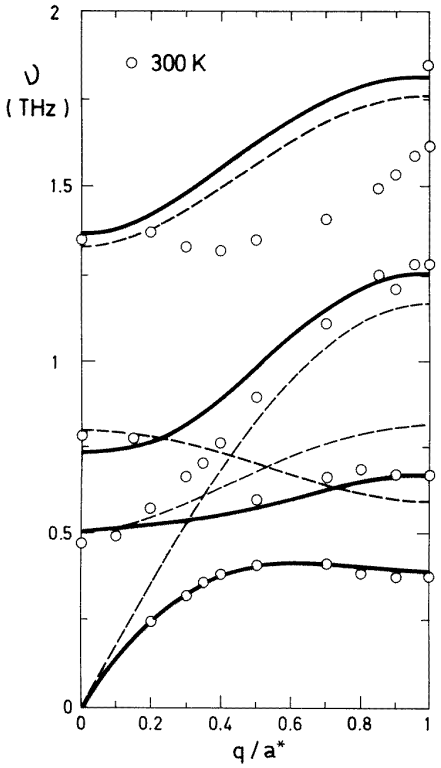

(c)

Figure 7. (Continued)

frequencies of $B_{2u}(L)$, $B_{1g}(L)$, $B_{3g}(L)$ and $A_u(L)$ as obtained from inelastic neutron scattering (for $B_{2u}(L)$ and $A_u(L)$) and from Raman scattering (for $B_{1g}(L)$ and $B_{3g}(L)$) we have found that all three intercolumn coupling constants show rather weak temperature dependences, roughly six or seven times weaker than for r_0 one (see table 4).

Table 4. Temperature derivatives of the squared frequencies of the optic modes and of the force constants r_0, r_1, r_a, r_c, t_a and t_c. The r_0 'self'-coupling constant shows a larger temperature dependence than all other coupling constants do.

	$(\partial/\partial T)\omega^2$ $(4\pi^2 10^{-5}$ THz^2 K$^{-1})$		$(\partial/\partial T)r_i$ $(4\pi^2 10^{-5}$ THz^2 K$^{-1})$
$B_{2u}(L)$	152	r_0	90
$A_u(L)$	56	r_1	14
$B_{1g}(L)$	72	r_a	11
$B_{3g}(L)$	80	r_c	13
$B_{1g}(T)$	−36	t_a	−9
$B_{3g}(T)$	−100	t_c	−25

We may thus conclude the following.

(i) the principal unstable degree of freedom in BCCD corresponds to the 'easy' rotations of betaine molecules and Ca complexes $CaCl_2 \cdot 2H_2O$, correlated along the b direction.

(ii) The anharmonic potential renormalizing the quasi-harmonic frequency associated with this degree of freedom arises essentially from intracolumn interactions.

4.4. The relevant anharmonic terms

The next important element necessary for the description of the mechanism of the soft-mode phase transition is the nature of the anharmonic terms responsible for the soft-mode temperature dependence. For a weakly anharmonic crystal, there are three contributions to the quasi-harmonic phonon frequencies in the lowest order in perturbation: the renormalization due to the quartic and cubic terms, and the contribution from linear coupling to the thermal strains [26]. In this section the role of these mechanisms in BCCD is briefly discussed.

The importance of the coupling to strains in BCCD was demonstrated experimentally by the pronounced effect of external pressure on the phase diagram of this compound [27]. Nevertheless, it appears that the role of thermal strain on the normal-incommensurate transition is only a secondary effect. Let us consider the strain dependence of the soft-mode quasi-harmonic frequency $\omega_{soft\ mode}$ explicitly:

$$\omega^2_{soft\ mode} = \text{function}[T, \epsilon_i(T)]. \tag{4.7}$$

Then the temperature derivative can be written as

$$\frac{\mathrm{d}}{\mathrm{d}T}(\omega^2_{soft\ mode}) \doteq A_T + A_\epsilon$$

with

$$A_T = \left(\frac{\partial}{\partial T}(\omega^2_{soft\ mode})\right)_\epsilon \qquad A_\epsilon = \sum_{i=1}^{3} \alpha_i \left(\frac{\partial}{\partial \epsilon_i}(\omega^2_{soft\ mode})\right)_T \tag{4.8}$$

where A_T stands essentially for the contribution of the quartic anharmonic terms (cubic terms formed only from the variables $\xi_n, \eta_{n+1}, x_n, \ldots$, being antisymmetric with respect to the σ_y mirror plane, are not allowed by symmetry) and A_ϵ is the contribution depending on the longitudinal thermal strain coefficients

$$\alpha_i = \frac{\partial \epsilon_i}{\partial T}$$

(the shear strains are zero owing to the orthorhombic symmetry).

The strain dependence of the quasi-harmonic frequency of the soft mode may be related to the strain dependence of the transition temperature T_i [28]. Rewriting 4.7 as $\omega^2_{soft\ mode} = A(T - T_i(\epsilon_i))$ we obtain the expression for the thermal strain contribution to the total soft-mode renormalization as

$$\frac{A_\epsilon}{A_\epsilon + A_T} \doteq \left[1 + 1 \Big/ \sum_{i=1}^{3} \left(\alpha_i \frac{\partial T_i}{\partial y(-\epsilon_i)}\right)\right]^{-1}. \tag{4.9}$$

By considering the values of $\partial T_i/\partial(-\epsilon_i)$ (1289, 1090 and 840 K) obtained from uniaxial external pressure experiments [29] and values of α_i (64.7, 60.9 and -13.3×10^{-6} K^{-1}) obtained from thermal dilatation measurements [24] we find that this thermal strain contribution represents only about 12% in the total soft-mode temperature dependence. Estimates for $\partial T_i/\partial(-\epsilon_i)$ compatible with those provided in the work of Kirchner *et al* [29] may be obtained also from the value of $\Delta C_p \doteq 0.066$ J cm^3 K^{-1} known from calorimetric

measurements [30], using the known values of the jumps of $\Delta\alpha_i$ [24], in a way similar to that used in [31] for K_2SeO_4.

Then it may be concluded that the soft-mode temperature renormalization arises primarily because of the quartic anharmonic terms, either owing to the simplest on-site terms

$$\xi_n^4 + \eta_n^4$$

which would renormalize only the parameter r_0, or perhaps owing to some more complicated terms such as

$$\xi_n^2\eta_n^2$$
$$\xi_n\eta_n(\xi_n^2 + \eta_n^2)$$

or

$$\xi_n^2\xi_{n+1}^2 + \eta_n^2\eta_{n+1}^2$$
$$\xi_n\xi_{n+1}(\xi_n^2 + \xi_{n+1}^2) + \eta_n\eta_{n+1}(\eta_n^2 + \eta_{n+1}^2)$$

that may simultaneously renormalize also r_a or r_c, respectively.

The remaining discrepancies may arise either because of the limited number of degrees of freedom (only two degrees of freedom per 28-atom formula unit), or because of the limitation to nearest-neighbour interactions only. In particular the neglected dipole–dipole coupling between easy rotations on more distant columns might improve the model†. The dispersion of the fourth lowest branch in the $\boldsymbol{q} \parallel \boldsymbol{a}^*$ data clearly does not fit well with the model proposed, while the frequency of the mode at 1.8 THz corresponds well to the calculated A_u mode even though this frequency was not taken into account when the coupling parameters were determined‡. We thus propose that the dispersion of the fourth branch in the $\boldsymbol{q} \parallel \boldsymbol{a}^*$ direction is not affected by the mixing with some other degree of freedom not taken into account in the model.

One of the most important microscopic assumptions of the present model is that there are exact correlations between the introduced 'easy' displacements performed by the entities belonging to the same 'column'. For the case of rotational degrees of freedom this assumption is well corroborated by the experimental fact that the dispersion of the related optic branch is relatively small in the a^* and c^* directions compared with the b^* direction.

Note that some *other* degrees of freedom may be preferentially correlated for example within the zigzag chains parallel to the direction a or inside the 'layers' around the σ_c symmetry elements, but our experimental results showed that this is not the case for those two degrees of freedom involved in the lowest-frequency modes investigated here.

From the phenomenological point of view the model can be viewed as a mode-mixing scheme. As in the case of quartz or K_2SeO_4, the appearance of the minimum on the lowest branch at a general value of the phonon wavevector is clearly linked to the coupling between the acoustic and the unstable optic branch. In the present model (as in the recent work of Kappler and Walker [22]), coupling to other branches is introduced, too. These

† We have checked that the introduction of the next-neighbour interaction improves the agreeement with the experimental dispersions along a^*. It also shifts the position of the minimum on the soft branch closer to $q_s = c^*/3$. The same effect was obtained also via the introduction of the approximate correction proposed by Smirnov [32].

‡ The agreement for the latter mode can be understood as a consequence of the relation (3.21). By inspection of the dynamical matrix it can be shown that this relation is directly linked with the fact that there is no coupling or only a small coupling between the translations of formula units belonging to columns related by the C_{2b} operation. The most probable microscopic explanation of this fact is that the coupling between the translational degrees of freedom is given primarily by the hydrogen bonds, which link only the nearest-neighbour columns related by σ_a and σ_c.

supplementary branches appear here naturally owing to the formulation of the model in terms of column variables, as a consequence of the assumption that there are four formula units per unit cell, each described by an independent variable. We have found that in fact the most convenient description of the lowest branch *demands* a scheme with simultaneous mixing between at least two 'rotational' branches and one translational (acoustic) branch.

Let us illustrate this statement in a different way. It might seem from section 3 (or from the formal construction of layer modes provided in [8, 22]) that the symmetry-adapted extended bare branches of Λ_3–Λ_2 symmetry in the Pnma structure have to connect the B_{2u} mode with the B_{1g} mode, and the B_{3g} mode with the A_u mode. In fact this is not necessarily so; the alternative definition of the symmetry-adapted extended bare Λ_3–Λ_2 branches (that connect B_{2u} with A_u, and B_{3g} with B_{1g}) is equally possible. Indeed, if we define

$$\eta'_n = \eta_{n-1}$$

the complex Fourier transform of the variables

$$\phi'_n = \frac{\xi_n + \eta'_n}{\sqrt{2}} = \frac{\xi_n + \eta_{n-1}}{\sqrt{2}} \qquad \psi'_n = \frac{\xi_n - \eta'_n}{\sqrt{2}} = \frac{\xi_n - \eta_{n-1}}{\sqrt{2}}$$

defined by analogy with (3.1), may be viewed as collective coordinates with respect to symmetry-adapted bare modes $\{|\phi'(q)\rangle, |\psi'(q)\rangle\}$, that fulfil the above-mentioned symmetry conditions:

(i) $|\phi'(0)\rangle$ belongs to the B_{2u} representation;
(ii) $|\psi'(0)\rangle$ belongs to the B_{3g} representation;
(iii) $|\phi'(1)\rangle$ belongs to the A_u representation;
(iv) $|\psi'(1)\rangle$ belongs to the B_{1g} representation.

The dispersion of these bare modes is now given by the expressions

$$\begin{aligned} D_{\phi'\phi'} &= b_{B_{2u}} + (b_{A_u} - b_{B_{2u}}) \sin^2\left(\frac{\pi q}{2}\right) \\ D_{\psi'\psi'} &= b_{B_{1g}} \ + \ (b_{B_{3g}} - b_{B_{1g}}) \cos^2\left(\frac{\pi q}{2}\right) \end{aligned} \tag{4.10}$$

and their direct interaction is given by

$$D_{\phi'\psi'} = -2\,\mathrm{i} r_a \sin(\pi q).$$

The dispersions of such '*flat*' bare branches are in fact closer to the resulting eigenmodes (see figure 4) and their mutual coupling is also much smaller than in the case of the branches $\{|\phi(q)\rangle, |\psi(q)\rangle\}$. Therefore, in this sense, the mixing scheme with the alternative 'flat' bare branches provides a more natural description than the previous description. The interaction terms with the acoustic branch $|u(q)\rangle$ have now a slightly more complex form

$$\begin{aligned} D_{u\phi'} &= \mathrm{e}^{(i\pi q/2)} \cos\left(\frac{\pi q}{2}\right)\left[(-2d_c + d_{B_{1g}}) \sin^2\left(\frac{\pi q}{2}\right)\right] \\ D_{u\psi'} &= \mathrm{i}\,\mathrm{e}^{(i\pi q/2)} \sin\left(\frac{\pi q}{2}\right)\left[-2d_c \cos^2\left(\frac{\pi q}{2}\right) - d_{B_{1g}} \sin^2\left(\frac{\pi q}{2}\right)\right]. \end{aligned} \tag{4.11}$$

The problem of coupling between the acoustic and optic branches can now be re-examined. The change in the sign of $D_{u\phi'}$ does not alter substantially the dispersion in this case (unlike in the previously discussed case where the sign of $D_{u\phi}$ was changed). Nevertheless, it does not mean that the dispersion of the lowest branch can be well estimated when the interaction $D_{u\psi'}$ of the second optic branch with the acoustic branch is neglected. It appears that the simultaneous mixing of all three branches is again important here. It can be understood if the small magnitude of the mixing term $D_{u\phi'}$ is considered; at $q \approx 0.15c^*$

we obtained $|D_{u\phi'}| \approx 0.01(4\pi^2\ \mathrm{THz}^2)$ while the experimental value of the anticrossing gap is $\delta\omega^2 \approx \omega_2^2(0.15) - \omega_1^2(0.15) \approx 0.1(4\pi^2\ \mathrm{THz}^2)$. (Let us recall that $\delta\omega^2 = 2|D_{u\phi'}|$ would hold in the case of the simple pair mixing.)

On the other hand, $|D_{u\psi'}|$ is sufficiently large and it is clearly responsible for the second anticrossing gap (at $q \approx 0.3c^*$, between $|\psi'(q)\rangle$ and $|u(q)\rangle$). The pair mixing relation $\delta\omega^2 = 2|D_{u\psi'}(0.3)|$ is well fulfilled in this case.

In other words, it seems that the necessity of including of the coupling with the second optic branch in the model for BCCD is linked mainly with the fact that the coupling of the acoustic branch with the lowest bare optic branch is quite small compared with the coupling of the acoustic branch with the second bare optic branch. This result is given by the *q dependence* of the two coupling terms rather than by the specific values of the mixing parameters, and it is therefore independent of the choice for the bare vectors (both $D_{u\phi'}$ and $D_{u\phi}$ behave as q^2 for small q vectors, while $D_{u\phi'}$ and $D_{u\phi}$ are proportional to q for small q vectors).

Finally, if $d_{B_{1g}}$ and $d_{B_{3g}}$ are not too large, the pair mixing relation $\delta\omega^2 = 2|D_{u\psi'}(0.3)|$ for the second anticrossing gap may in fact be taken as the ninth condition on the values of the coupling parameters.

The value of this gap can be well estimated directly from the experimental data

$$\delta\omega^2 \approx \omega_3^2(0.3) - \omega_1^2(0.3) \approx 0.22\ (4\pi^2\ \mathrm{THz}^2)$$

while its value would, in the case of purely pair mixing, be given by

$$2|D_{u\psi'}(0.3)| \approx 0.454\,|1.59d_c + 0.206d_{B_{1g}}|\ (4\pi^2\ \mathrm{THz}^2). \tag{4.12}$$

This approximate condition enables one to explain why only the choices with opposite signs for $d_{B_{1g}}$ and d_c could provide satisfactory fits to the experimental dispersion curves; the experimental value of this anticrossing gap is rather small so that, without compensation of the two terms in (4.12), the agreement could not be achieved.

In conclusion, we may state that the mechanism for the appearance of the incommensurate phase in BCCD is due to the competing interactions between different degrees of freedom, in the sense of the original proposal of Axe *et al* [18] and the related approaches developed subsequently for example in [33, 34] and that the above model provides a quantitative description of these interactions in the present compound.

5. Conclusion

A simple microscopic lattice dynamical model for BCCD was constructed, starting from the following assumptions.

(i) The lowest-frequency branches of Λ_3 and Λ_2 symmetry involve only two distinct degrees of freedom per formula unit.

(ii) Displacements related to these degrees of freedom are highly correlated along chains of betaines and Ca complexes ($CaCl_2 \cdot 2H_2O$) parallel to the b direction.

Even though we were not able to find a unique set of coupling constants from a comparison with the experimental dispersion curves, several semi-quantitative conclusions could be obtained about the mechanism of the normal–incommensurate transition.

First, the existence of a dispersion minimum on the Λ_3 branch and its non-existence on the Σ_4 branch (leading to the appearance of the modulation along the $\boldsymbol{q} \parallel \boldsymbol{c}^*$ direction) were ascribed to the difference in the signs of the translational–rotational intercolumn coupling constants. This is possibly due to the simultaneous mixing between more than two branches.

Secondly, it could be established that the most important temperature effect concerns the intracolumn quasi-harmonic coupling constant describing the stiffness of the single column itself with respect to the characteristic librational degree of freedom (‘easy rotation’).

Finally, it was verified that the temperature dependence of this coupling constant is not related to the thermal strain. The most probable (i.e. lowest-order) anharmonic terms that give rise to such renormalization are the quartic anharmonic on-site potentials for the easy rotation column variables. This conclusion strongly supports the physical relevance of the generalized DIFFOUR model for the description of the BCCD crystal. Furthermore, we wish to emphasize that the coupling of the soft branch with another low-frequency branch is crucial for the appearance of the incommensurate instability. We have argued that, as long as the coupling among the critical librations of the four formula units is assumed to be weak, the simultaneous softening of the two Λ_3 branches is expected. We believe that a similar mechanism may account for the occurrence of the incommensurate instability in other structurally related dielectric crystals.

With respect to the model proposed recently by Kappler and Walker, our ten-parameter microscopic model is improved in several respects.

Our model is based on the assumption that both optic branches correspond to the same degree of freedom of the formula unit, while in the models of Kappler and Walker no relation between the two optic branches is assumed. The explicit microscopic interpretation that was given to the variables and then to the coupling terms in the present model allows a close comparison with neutron scattering results. The prediction of the present model concerning the dynamics of the incommensurate phase will be presented in a forthcoming publication and tested against Raman and neutron scattering data.

Acknowledgments

One of the authors (JH) wishes to thank Professor T Janssen and Professor V Dvořák for valuable discussions and to express his gratitude to the Laboratoire Léon Brillouin and Centre d’Etudes de Saclay, for providing the PhD scholarship as well as for hospitality and support throughout this work.

References

[1] Frenkel Y I and Kontorova T 1938 *Zh. Eksp. Teor. Fiz.* **8** 1340
[2] Frank F C and van der Merve J H 1949 *Proc. R. Soc.* A **198** 205
[3] Aubry S 1978 *Solitons and condensed Matter Physics* ed A R Bishop and T Schneider (Berlin: Springer) pp 264–77
[4] Selke W 1988 *Phys. Rep.* **170** 213
[5] Bak P and von Boehm J 1980 *Phys. Rev.* B **21** 5297
[6] Janssen T and Tjon J A 1982 *Phys. Rev.* B **25** 3767
[7] Tentrup T and Siems R 1990 *Ferroelectrics* **105** 379
[8] Chen Z Y and Walker M B 1991 *Phys. Rev.* B **43** 760
[9] Ao R and Schaack G 1988 *Indian J. Pure Appl. Phys.* **26** 124
[10] Pérez-Mato J M 1988 *Solid. State Commun.* **67** 1145
[11] Brill W, Schildkamp W and Spilker J 1985 *Z. Kristallogr.* **172** 281
[12] Dvořák V 1990 *Ferroelectrics* **104** 135
[13] Volkov A A, Goncharov Yu G, Kozlov G V, Albers J and Petzelt J 1986 *JETP Lett.* **44** 603
[14] Ao R and Schaack G 1988 *Ferroelectrics* **80** 105
[15] Goncharov Yu G, Kozlov G V, Volkov A A, Albers J and Petzelt J 1988 *Ferroelectrics* **80** 221
[16] Currat R, Legrand J F, Kamba S, Petzelt J, Dvořák V and Albers J 1990 *Solid. State Commun.* **75** 545
[17] Zuniga F J, Ezpeleta J M, Pérez-Mato J M and Paciorek W 1991 *Phase Trans.* **31** 29
[18] Axe J D, Harada J and Shirane G 1970 *Phys. Rev.* B **1** 1227

[19] Dolino G, Berge B, Valade M and Moussa F 1992 *J. Physique I* **2** 1461
[20] Valade M, Berge B and Dolino G 1992 *J. Physique I* **2** 1481
[21] Hlinka J, Quilichini M, Currat R and Legrand J F 1996 *J. Phys.: Condens. Matter*
[22] Kappler C and Walker M B 1993 *Phys. Rev.* B **48** 5902
[23] Janssen T 1992 *Z. Phys.* B **86** 277
[24] Haussühl S, Liedtke J, Albers J and Klöpperpieper A 1988 *Z. Phys.* B **70** 222
[25] Etxebarria I, Quilichini M, Pérez-Mato J M, Boutrouille P, Zuniga F J and Breczewski T 1992 *J. Phys.: Condens. Matter* **4** 8551
[26] Bruce A D and Cowley R A 1981 *Structural Phase Transitions* (London: Taylor & Francis) p 86
[27] Ao R, Schaack G, Schmidt M and Zöller M 1989 *Phys. Rev. Lett.* **62** 183
[28] Gesi K 1992 *Phase Trans.* **40** 187
[29] Kirchner B, Le Maire M, Schaack G and Schmitt-Lewen M 1993 *Europhys. Lett.* **22** 113
[30] Brill W, Gmelin E and Ehses K H 1990 *Ferroelectrics* **103** 25
[31] Li Gen, Tao N, Le Van Hong, Cummins H Z, Dreyfus D, Hebbache M, Pick R M and Vagner J 1990 *Phys. Rev.* B **42** 4406
[32] Smirnov M 1989 *Solid State Commun.* **70** 403; 1993 *Solid. State Commun.* **86** 459
[33] Levanyuk A P and Sannikov D G 1976 *Sov. Phys.–Solid State* **18** 245
[34] McConnell J D C 1978 *Z. Kristall* **147** 45
Heine V and McConnell J D C 1984 *J. Phys. C: Solid State Phys.* **17** 1129
[35] Freitag O and Unruh H G 1990 *Ferroelectrics* **105** 357
[36] Ezpeleta J M, Zuniga F J, Pérez-Mato J M, Paciorek W and Breczewski T 1992 *Acta Crystallogr.* B **48** 261